CHAPTER 4

ROTATIONAL DYNAMICS OF RIGID AND MULTIPLE RIGID BODY SPACECRAFT

4.1 OVERVIEW

Here we present a significant body of analytical and numerical results which pertain to spacecraft modeled as either a single rigid body, or a rigid body containing symmetric rotors. The results presented for the single rigid body case are fundamental and near-classical, even though some of the results has been developed only during the past two decades.

4.2 TORQUE-FREE MOTION OF A SINGLE RIGID BODY

4.2.1 Energy and Momentum Integrals

We consider the dynamics of a general rigid body with arbitrary initial conditions. If external torques are negligible, we can uncouple the rotational motion. Two integrals of the rotational motion play a central role. From Eq. 3.25, it is clear that angular momentum is constant; this is true even for a nonrigid body or general collection of bodies, in the absence of external torques. From Eq. 3.43, it is evident that the kinetic energy of the motion is constant. For the case of a rigid body, we make use of Eqs. 3.24 and 3.40 to write these two integrals as quadratic functions of angular velocity and the principal inertias as

$$\textit{momentum ellipsoid:}\quad H^2 = I_1^2\omega_1^2 + I_2^2\omega_2^2 + I_3^2\omega_3^2 \tag{4.1}$$

$$\textit{energy ellipsoid:}\quad 2T = I_1\omega_1^2 + I_2\omega_2^2 + I_3\omega_3^2 \tag{4.2}$$

Thus, we have a geometrical interpretation for the torque-free motion angular velocity solution $\omega(t)$. Relative to body-fixed axes, $\omega(t)$ moves along the space curve intersection of the two ellipsoidal surfaces of Eqs. 4.1 and 4.2. Since these surfaces are both tri-axial ellipsoids, the family of intersection curves is difficult to visualize. The conceptual situation can be simplified by transforming both surfaces so that one of them is a sphere. This transformation is easily accomplished by using the momentum components H_i

$= I_i\omega_i$ in lieu of the angular velocity components as velocity coordinates; thus Eqs. 4.1 and 4.2 become

$$\textit{momentum sphere:} \quad H^2 = H_1^2 + H_2^2 + H_3^2 \tag{4.3}$$

$$\textit{energy ellipsoid:} \quad 1 = \frac{H_1^2}{2I_1T} + \frac{H_2^2}{2I_2T} + \frac{H_3^2}{2I_3T} \tag{4.4}$$

The semi axes of the energy ellipsoid are clearly ($\sqrt{2I_iT}$, $i = 1,2,3$). The curves of intersection of the ellipsoid Eq. 4.4, plotted on the sphere, Eq. 4.3 provide an elegant geometrical device for obtaining some significant qualitative information on the nature and limiting properties of large nonlinear motions.

To gain some useful insights, we consider angular momentum (H) to be a constant (e.g., for zero external torque), and sweep the kinetic energy (T) over all physically possible values. In order to obtain the upper and lower limits on T, we determine the maximum and minimum T satisfying Eq. 4.4, using Eq. 4.3 as a constraint. The most obvious way to maximize or minimize T (from Eq. 4.4) subject to H = constant is to solve Eq. 4.3 for one of (H_1, H_2, H_3) as a function of the other two and substitute into Eq. 4.4. Solving for H_1^2 as a function of H_2^2 and H_3^2, we find from Eq. 4.3

$$H_1^2 = H^2 - (H_2^2 + H_3^2) \tag{4.5}$$

Upon substituting Eq. 3.150 into Eq. 3.149, we find

$$T = \frac{H^2}{2I_1} + \frac{1}{2}\left(\frac{I_1-I_2}{I_1I_2}\right)H_2^2 + \frac{1}{2}\left(\frac{I_1-I_3}{I_1I_3}\right)H_3^2 \tag{4.6}$$

It is obvious by inspection that the extreme value of T is $H^2/(2I_1)$ and this is a maximum, minimum, or saddle point at $H_1 = \pm H$, $H_2 = H_3 = 0$ depending on the following:

(i) T has a maximum value at the state $H_1 = \pm H$, $H_2 = H_3 = 0$ if $I_1 < I_2$ and $I_1 < I_3$; thus *spin about the axis of minimum inertia is a maximum energy state.*

(ii) T has a minimum at the state $H_1 = \pm H$, $H_2 = H_3 = 0$ if $I_1 > I_2$ and $I_1 > I_3$; thus *spin about the axis of maximum inertia is a minimum energy state.*

(iii) T has a saddle point at the state $H_1 = \pm H$, $H_2 = H_3 = 0$ if ($I_1 > I_2$ and $I_1 < I_3$) or ($I_1 < I_2$ and $I_1 > I_3$); thus *spin about the axis of intermediate inertia is a saddle point energy state.*

Since T is a quadradic function of (H_2,H_3), the above local stationary points are obviously global, i.e., (i) and (ii) characterize the *global* maximum and minimum of T, subject to the constraint that Eq. 4.3 is satisfied (angular momentum is constant).

We can recast the above discussion if a specific ordering of axes is used. If we define the body fixed principal axes $(\hat{b}_1, \hat{b}_2, \hat{b}_3)$ so that the corresponding inertias have the fixed ordering

$$I_1 \geq I_2 \geq I_3$$

The above remarks require three critical energy values

$$T_1 = \frac{H^2}{2I_1} \quad [\textit{minimum energy} \text{ motion } (H_1 = \pm H,\ H_2 = H_3 = 0), \text{ spin about the largest inertia axis } \hat{b}_1]$$

$$T_2 = \frac{H^2}{2I_2} \quad [\textit{intermediate energy} \text{ motion } (H_2 = \pm H,\ H_1 = H_3 = 0), \text{ spin about the intermediate inertia axis } \hat{b}_2]$$

$$T_3 = \frac{H^2}{2I_3} \quad [\textit{maximum energy} \text{ motion } (H_3 = \pm H,\ H_1 = H_2 = 0), \text{ spin about the least inertia axis } \hat{b}_3]$$

Since the above extremum values of energy are seen to occur at specific, unique points, we anticipate that the intersections of Eq. 4.4 with Eq. 4.3 will contain these as limiting cases. Figure 4.1 depicts the energy/momentum

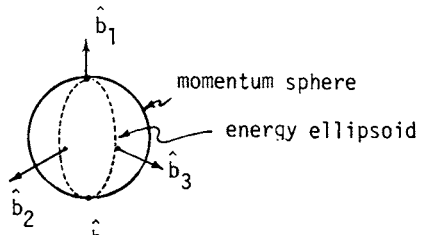

Fig. 4.1a Pure spin about axis of largest inertia, $T = T_{min} = \frac{H^2}{2I_1}$, energy ellipsoid totally within momentum sphere, tangent at $\pm H\hat{b}_1$.

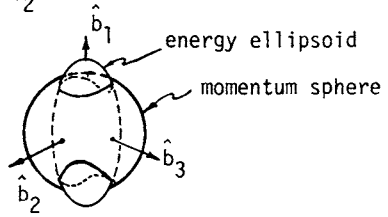

Fig. 4.1b Large nutational motions "near" spin about $\hat{b}_1$,

$$\frac{H^2}{2I_1T} < T < \frac{H^2}{2I_2T}$$

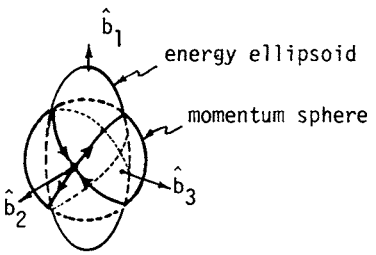

Fig. 4.1c Sepratrix case, motion for $T = \frac{H^2}{2I_2T}$, the ellipsoid is tangent to the sphere at $\pm H\hat{b}_2$. not spin about $\hat{b}_2$ is an unstable equilibrium.

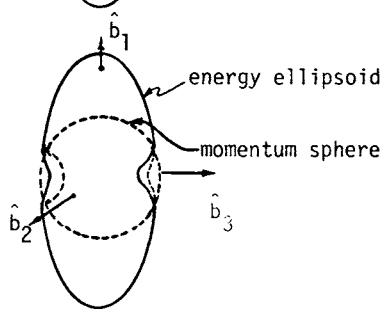

Fig. 4.1d Large nutational motions "near" spin about $\hat{b}_3$,

$$\frac{H^2}{2I_2T} < T < \frac{H^2}{2I_3T}.$$

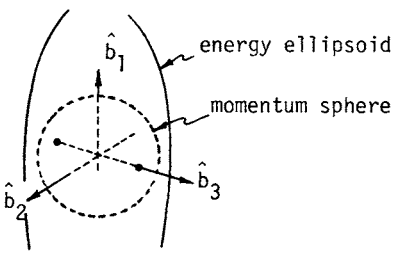

Fig. 4.1e Pure spin about axis of least inertia, $T = T_{max} = \frac{H^2}{2I_3T}$, momentum sphere totally within energy ellipsoid, tangent at $\pm H\hat{b}_3$.

Figure 4.1 Intersections of the Energy Ellipsoid and the Momentum Sphere

surface intersections for five energy values, including the above three extremes. For an intermediate energy value $\frac{H^2}{2I_1} < T < \frac{H^2}{2I_2}$, or $\frac{H^2}{2I_2} < T < \frac{H^2}{2I_3}$, the energy ellipsoid is partially "inside" and partially "outside" the momentum sphere, as depicted in Figures 4.1b-d. Note the sepratrix case, the momentum constrained energy saddle occurs at $T = \frac{H^2}{2I_2}$. The entire family of intersection curves is shown in the computer generated portrait of Figure 4.2.

It is worth emphasizing the following points regarding these intersection curves:

(i) Once initial conditions are specified (thereby establishing H and T as well as a starting point), the torque-free motion of a rigid body will theoretically evolve forever with the angular momentum vector tracing out a particular intersection curve. Excluding the sepratrix case ($H^2 = 2I_2T$), these curves are closed and are traversed with a finite period. As is shown by Morton and Junkins (ref. 1), the $H_i(t)$ and $\omega_i(t)$ (of which these intersection curves are the locus) are periodic elliptic functions whose period depends upon I_1, I_2, I_3, H^2, $2T$. Thus these intersection curves provide a geometrical interpretation of the three Jacobian elliptic functions (analogous to a circle or, more generally, an ellipse for circular trigonometric functions). The limiting sepratrix motion (for $H^2 = 2I_2T$) has an infinite associated period; the elliptic functions degenerate into hyperbolic functions, for this limiting case.

(ii) Recall **H** is fixed in inertial space, so from an inertial viewpoint, *these time varying projections of* **H** *onto the moving body axes are generated as a consequence of the body's motion* relative to the inertially constant **H** vector.

In practical applications, one often finds a heuristic approach to attitude stability useful. For "quasi-rigid" bodies, small intended or

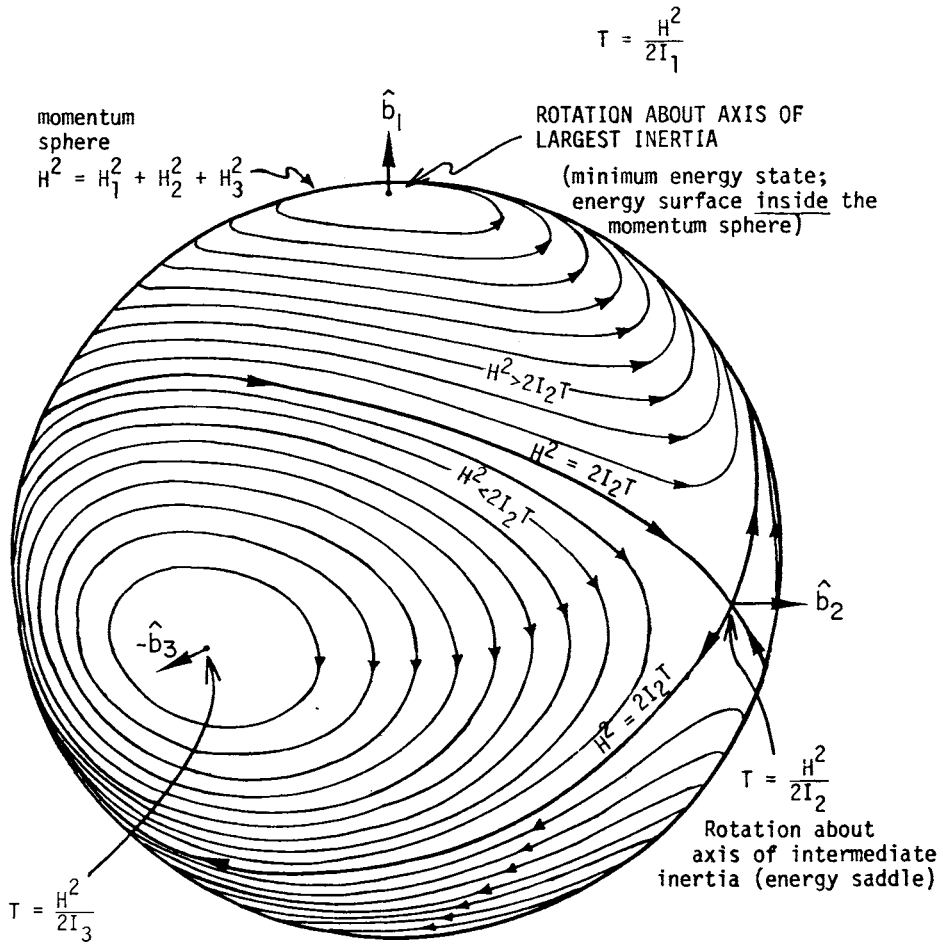

Figure 4.2 The Family of Energy/Momentum Intersection Trajectories for Torque-Free Motion

unintended departures from rigidity result in internal energy dissipation (for example, mechanical energy transformed into heat). If the external torques are zero, **H** is constant regardless of the internal processes and the degree of rigidity. Thus, it seems reasonable to artificially reduce the energy T while holding **H** constant. This "energy sink" approach, even heuristicly applied, does usually lead to correct results. This heuristic energy sink argument immediately leads, for example, to the conclusion that the only stable state is pure spin about the axis of largest inertia (which is the global minimum energy state for constant angular momentum). A significant fraction of spacecraft in orbit today are spinning stably about their axis of largest inertia, and of course, the earth, moon, sun, and all of the planets (whose spin and inertia have been determined) are natural examples of bodies spinning about their axes of largest inertia, to a high degree of approximation. Despite the fact that Lagrange and others in the 1800's knew that a "spin stabilized" body should be spun about the axis of largest inertia, Explorer 1 was spun about its axis of least inertia - it began tumbling after a fraction of the first orbit! Since completion of the Explorer 1 post-flight analysis, dynamicists have enjoyed a more influential role in pre-flight studies and mission analysis aspects of our space program!

The heuristic energy sink approach can also lead to incorrect results. When we are ignoring the specific internal process dynamics in writing the energy and momentum expressions, we run a risk that the ignored degrees of freedom will couple in some unexpected, perhaps destabilizing, way with the motions of interest. For example, we find in Section 4.4 and Ref. [10] that a rigid spacecraft containing a rigid flywheel can be stablized about any body fixed axis, a physically comfortable result, but it is not predicted by ignoring the flywheel and making a heuristic application of the energy sink idea for a single rigid body. References 2, 3, place the energy sink

approach upon a firm analytical foundation and demonstrate that erroneous results are more often obtained when the approach is incorrectly applied!

4.2.2 Nonlinear Oscillator Analog of Rigid Body Motion

A very closely related geometrical device (to the momentum/energy surface intersections) is the nonlinear oscillator analog developed by Junkins, Jacobson, and Blanton (ref. 4). We now summarize the principal features of this analog. Euler's equations 3.31 for the torque-free case and principal axes are

$$\begin{aligned} I_1\dot{\omega}_1 &= (I_2 - I_3)\omega_2\omega_3 \\ I_2\dot{\omega}_2 &= (I_3 - I_1)\omega_3\omega_1 \\ I_3\dot{\omega}_3 &= (I_1 - I_2)\omega_1\omega_2 \end{aligned} \tag{4.7}$$

The momentum and energy equations (Eqs. 4.1 and 4.2) are exact integrals of these equations. Clearly Eqs. 4.1 and 4.2 can be considered two equations in the three unknown $\omega_i(t)$; any pair of ω_i's can be solved as a function of the third. The three possible solutions are

$$\left.\begin{aligned} \omega_2^2 &= \left(\frac{2I_3T - H^2}{I_2I_3 - I_2^2}\right) - \left(\frac{I_1I_3 - I_2^2}{I_2I_3 - I_2^2}\right)\omega_1^2 \\ \omega_3^2 &= \left(\frac{2I_2T - H^2}{I_2I_3 - I_3^2}\right) - \left(\frac{I_1I_2 - I_1^2}{I_2I_3 - I_3^2}\right)\omega_1^2, \end{aligned}\right\} \tag{4.8a}$$

$$\left.\begin{aligned} \omega_1^2 &= \left(\frac{2I_3T - H^2}{I_1I_3 - I_1^2}\right) - \left(\frac{I_2I_3 - I_2^2}{I_1I_3 - I_1^2}\right)\omega_2^2 \\ \omega_3^2 &= \left(\frac{H^2 - 2I_1T}{I_3^2 - I_1I_3}\right) - \left(\frac{I_2^2 - I_1I_2}{I_3^2 - I_1I_3}\right)\omega_2^2, \end{aligned}\right\} \tag{4.8b}$$

$$\left.\begin{aligned} \omega_1^2 &= \left(\frac{2I_2T - H^2}{I_1I_2 - I_1^2}\right) - \left(\frac{I_2I_3 - I_3^2}{I_1I_2 - I_1^2}\right)\omega_3^2 \\ \omega_2^2 &= \left(\frac{H^2 - 2I_1T}{I_2^2 - I_1I_2}\right) - \left(\frac{I_3^2 - I_1I_3}{I_2^2 - I_1I_2}\right)\omega_3^2. \end{aligned}\right\} \tag{4.8c}$$

These three sets of equations prove useful in uncoupling Euler's Eq. 4.7. Differentiation of Euler's equations yields

$$\ddot{\omega}_1 = \left(\frac{I_2 - I_3}{I_1}\right)(\dot{\omega}_2\omega_3 + \omega_2\dot{\omega}_3) \tag{4.9a}$$

$$\ddot{\omega}_2 = \left(\frac{I_3 - I_1}{I_2}\right)(\dot{\omega}_3\omega_1 + \omega_1\dot{\omega}_3) \tag{4.9b}$$

$$\ddot{\omega}_3 = \left(\frac{I_1 - I_2}{I_3}\right)(\dot{\omega}_1\omega_2 + \omega_1\dot{\omega}_2). \tag{4.9c}$$

and substitution of Eq. 4.7 into the right hand sides of Eq. 4.9 to eliminate the $\dot{\omega}$'s yields

$$\ddot{\omega}_1 = \left(\frac{I_2 - I_3}{I_1}\right)\left\{\left(\frac{I_1 - I_2}{I_3}\right)\omega_1\omega_2^2 + \left(\frac{I_3 - I_1}{I_2}\right)\omega_1\omega_3^2\right\} \tag{4.10a}$$

$$\ddot{\omega}_2 = \left(\frac{I_3 - I_1}{I_2}\right)\left\{\left(\frac{I_1 - I_2}{I_3}\right)\omega_1^2\omega_2 + \left(\frac{I_2 - I_3}{I_1}\right)\omega_2\omega_3^2\right\} \tag{4.10b}$$

$$\ddot{\omega}_3 = \left(\frac{I_1 - I_2}{I_3}\right)\left\{\left(\frac{I_3 - I_1}{I_2}\right)\omega_1^2\omega_3 + \left(\frac{I_2 - I_3}{I_1}\right)\omega_2^2\omega_3\right\} \tag{4.10c}$$

Finally, substitution of Eq. 4.8a, b, c, respectively, into Eq. 4.10a, b, c yields the remarkable result

$$\ddot{\omega}_i + A_i\omega_i + B_i\omega_i^3 = 0 \; ; \; i = 1,2,3, \tag{4.11}$$

where the constants $\{A_1,B_1 \; ; \; A_2,B_2 \; ; \; A_3,B_3\}$ are functions of $(I_1,I_2,I_3,2T,H^2)$, given in Table 4.1. Equations 4.11 are seen to be examples of homogeneous, undamped Duffings' equations, encountered often in analysis of nonlinear oscilations (refs. 4,5). In nonlinear mechanical oscillations, the cubic "stiffness" term usually arises to approximately account for a nonlinear departure from Hooke's linear spring model. In the present case, Eqs. 4.11 are *exact* differential equations governing the angular velocity components for torque free motion of a general rigid body. Equations 4.11 can be employed to

define three *uncoupled* non-linear oscillators. Notice that while the oscillators are *uncoupled*, they are not *independent*. The six spring constants are all uniquely determined from initially evluated inertia, energy, and momentum constants. It is interesting to note (Table 4.1) that the spring constants (B_1,B_2,B_3) are independent of both energy and momentum; the nonlinear spring is a function *only* of inertia properties. Each of these oscillators is an analog for one component of the motion and, since Eqs. 4.11 are uncoupled, the three angular velocity components can be rigorously defined and analyzed as a nonlinear oscillator.

The oscillator analog differential equations of Eqs. 4.11 have three immediate integrals of the form

$$\dot{\omega}_i^2 + A_i\omega_i^2 + \frac{B_i}{2}\omega_i^4 = K_i \quad , \quad i = 1,2,3, \tag{4.12}$$

where (K_1, K_2, K_3) are three oscillator 'energy-type' integral constants of the motion (we conclude that 'energy' (K_i) is conserved in each of the three angular velocity/angular acceleration spaces). Equation 4.12 thus defines a family of integral curves in each ω_i, $\dot{\omega}_i$ space which depends upon A_i, B_i, and

TABLE 4.1

'SPRING CONSTANTS' OF THE NONLINEAR OSCILLATOR ANALOG

i	A_i	B_i
(1)	$\frac{(I_1 - I_2)(2I_3T - H^2) + (I_3 - I_1)(H^2 - 2I_2T)}{I_1I_2I_3}$	$\frac{2(I_1 - I_2)(I_1 - I_3)}{I_2I_3}$
(2)	$\frac{(I_2 - I_3)(2I_1T - H^2) + (I_1 - I_2)(H^2 - 2I_3T)}{I_1I_2I_3}$	$\frac{-2(I_1 - I_2)(I_2 - I_3)}{I_1I_3}$
(3)	$\frac{(I_3 - I_1)(2I_2T - H^2) + (I_2 - I_3)(H^2 - 2I_1T)}{I_1I_2I_3}$	$\frac{2(I_1 - I_3)(I_2 - I_3)}{I_1I_2}$

K_i for their characterization. The constants (K_1,K_2,K_3) can be evaluated in terms of physical parameters by substituting from Eq. 4.7 to obtain (after considerable algebra) the results

$$K_1 = \frac{(2I_2T - H^2)(H^2 - 2I_3T)}{I_1^2 I_2 I_3} \tag{4.13a}$$

$$K_2 = \frac{(2I_3T - H^2)(H^2 - 2I_1T)}{I_1 I_1^2 I_3} \tag{4.13b}$$

and

$$K_3 = \frac{(2I_1T - H^2)(H^2 - 2I_2T)}{I_1 I_2 I_3^2} \tag{4.13c}$$

By inspection of the oscillator analog constants, Eqs. 4.13 and Table 4.1, it is clear that each specification of values for I_1, I_2, I_3, $2T$, H^2 directly specifies particular values for the "energy" and "spring" constants in the oscillator analog. This gives rise to a unique situation in which any change in the 'energy' (K_i) of either of the oscillators (resulting from varying one of more of the physical constants I_1, I_2, I_3, $2T$, H^2) requires a corresponding change in the 'spring' constants (A_i and B_i). In a simple nonlinear oscillator, the energy constant can be varied while holding the spring constants fixed; giving rise to a family of iso-energy phase trajectories (in displacement/velocity space), which do not cross. In the case at hand, sweeping any one of the physical variables (I_1, I_2, I_3, $2T$, H^2) generates a family of phase trajectories (in each of the three ω, $\dot{\omega}$ spaces) which may (in general) cross. These three planes will be seen to provide an important analytical tool in rigid body dynamics. Their properties are developed below.

If we adopt an ordering of principal axes so that $I_1 \geq I_2 \geq I_3$, it can be established that the "spring constants" from Table 4.1 satisfy the inequalities

$$A_1 \gtrless 0 \quad , \quad B_1 > 0$$

$$A_2 > 0 \quad , \quad B_2 < 0 \tag{4.14}$$

$$A_3 \gtrless 0 \quad , \quad B_3 > 0.$$

The following qualitative observations may prove useful in interpreting the developments which follow:

(1) The linear 'spring constants' (A_1, A_3) for the first and third oscillators can produce 'de-stabilizing spring forces' (a negative spring effect).

(2) The positive cubic 'spring constants' (B_1, B_3) for the first and third oscillators always produce 'restoring forces' and are therefore 'hard springs'. Since the cubic spring will always override the linear spring (for sufficiently large 'displacements') we could immediately hypothesize that all trajectories of the first and third phase planes must be closed.

(3) The cubic spring constant (B_2) for the second oscillator produces a 'destabilizing force' (and therefore corresponds to a 'soft spring'). Since the 'destabilizing cubic spring force' will eventually override the 'stabilizing linear spring force', we could hypothesize that (without imposing physical restrictions) the second oscillator differential equation could admit open phase trajectories.

The second oscillator (having the 'soft spring', and apparently admitting both open and closed trajectories) will be discussed first.

The phase plane trajectories of the second oscillator are defined by

$$\dot{\omega}_2^2 + A_2\omega_2^2 + \frac{B_2}{2}\omega_2^4 = K_2. \tag{4.15}$$

It is clear that, for ω_2 sufficiently small (so that ω_2^4 is negligible compared to ω_2^2) that Eq. 4.15 defines elliptical trajectories in ω_2, $\dot{\omega}_2$ space with semiaxes ($\sqrt{K_2}$, $\sqrt{K_2 A_2}$). We therefore conclude that 'small oscillations' in ω_2, $\dot{\omega}_2$ space are closed trajectories. In general, the $\dot{\omega}_2$ and ω_2 intercepts follow directly from Eq. 4.15 as

$$\dot{\omega}_2 \text{ (for } \omega_2 = 0) = \pm \sqrt{K_2} \tag{4.16}$$

and

$$\omega_2^2 \text{ (for } \dot{\omega}_2 = 0) = \frac{-A_2 \pm \sqrt{A_2^2 + 2B_2K_2}}{B_2}. \tag{4.17}$$

For closed trajectories in ω_2, $\dot{\omega}_2$ space, it is clearly necessary that the intercepts be real; we therefore conclude that it is necessary that

$$K_2 > 0 \tag{4.18}$$

and

$$F_2 \equiv A_2^2 + 2B_2K_2 > 0. \tag{4.19}$$

The positive sign of Eq. 4.17 must necessarily correspond to the closed trajectories about the origin, since it is known a priori that the closed curves are symmetric about the origin for ω_2 small. The negative sign locates the ω-intercepts of a family of hyperbola-like open trajectories (see Figure 4.3). Since the solutions for angular velocities and accelerations are known to be periodic, it is easy to conjecture that only the closed trajectories (in the shaded region of Figure 4.3) are physically possible. To establish this fact analytically, it is necessary to establish that violation of either of the conditions, Eq. 4.18 or Eq. 4.19, requires some physically inadmissible initial state. The non-negative character of K_2 is easily established by inspection of Eq. 4.13b, noting from Eqs. 4.1 and 4.2 that

$$(H^2 - 2I_3T) \equiv I_1(I_1 - I_3)\omega_1^2 + I_2(I_2 - I_3)\omega_2^2 \tag{4.20}$$

and

$$(2I_1T - H^2) \equiv I_2(I_1 - I_2)\omega_2^2 + I_3(I_1 - I_3)\omega_3^2 \tag{4.21}$$

are both positive semi-definite. Establishing that Eq. 4.19 is non-negative is more tedious, but it can be shown by substitution of K_2 from Eq. 4.13b and (A_2, B_2) from Table 4.1 (after considerable algebra) that

$$F_2 = \left(\frac{(I_1 - I_3)(H^2 - 2I_2T)}{I_1I_2I_3}\right)^2, \tag{4.22}$$

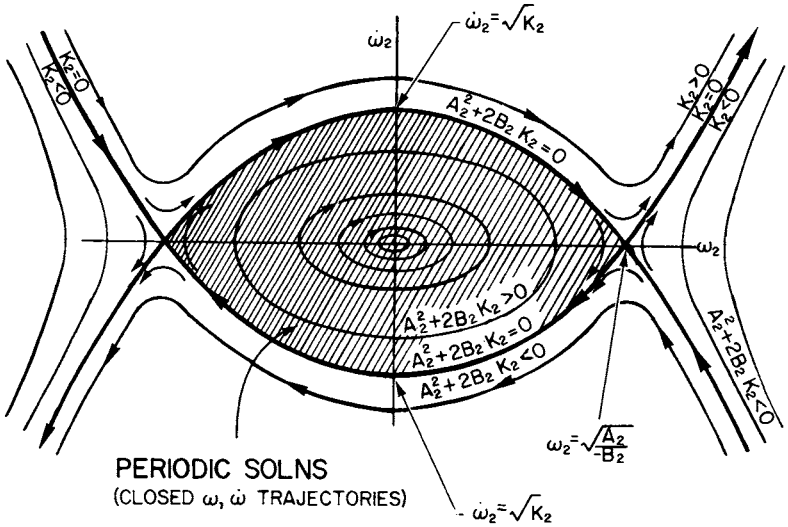

Figure 4.3 The ω_2, $\dot{\omega}_2$ Phase Plane

from which it clearly follows that $F_2 > 0$ for all physically admissible values of I_1, I_2, I_3, H^2, $2T$ (i.e. they must all be real numbers). The above analysis establishes that only the closed trajectories of Figure 4.3 are admissible in torque-free rigid body dynamics. Notice that the limiting trajectories approaching the periodic solution boundary occurs ($F \to 0$) when any of the three conditions occur:

$$I_1 \to I_3 \tag{4.23a}$$

$$H^2 \to 2I_2T \tag{4.23b}$$

$$I_1I_2I_3 \to \infty, \tag{4.23c}$$

Further, note that the second condition ($H^2 = 2I_2T$) defines the transition boundary between the two branches of the classical solution (see ref. 1) for angular velocities. We therefore conclude that all trajectories for cases

($H^2 > 2I_2T$) and ($H^2 < 2I_2T$) are closed trajectories contained interior to the periodic solution boundary curve whereas the 'degenerate case' ($H^2 = 2I_2T$) is the boundary (sepratrix) curve.

In analyzing the spacing of equal-time-interval-markers along the trajectories, we find that wide spacing occurs near the ends of the minor axes of the ω_2, $\dot{\omega}_2$ phase curves, while closest spacing occurs at the ends of the major axes. The spacing of equal time markers along the sepratrix trajectory for ($H^2 = 2I_2T$) in fact approaches zero as ω_2 approaches its maximum value (i.e., a condition of 'pure-spin' about $\hat{b}_2$ is approached in the limit as time goes to infinity). Notice (Figure 4.3) the one-sided character of the instability of pure spin about $\hat{b}_2$. A small positive change in $\dot{\omega}_2$ will result in asymptotic return to pure spin about $\hat{b}_2$; whereas a small negative change in $\dot{\omega}_2$ results in a hyperbolic departure from spin about $\hat{b}_2$, the body will asymptotically approach to a condition of pure spin about $-\hat{b}_2$.

The corresponding phase plane trajectories in the (ω_1, $\dot{\omega}_1$ and ω_3, $\dot{\omega}_3$) spaces can be obtained in an analogous fashion. The discussion is greatly simplified since, for 'hard spring oscillators', only closed trajectories theoretically exist. The phase trajectories for these spaces are defined by

$$\dot{\omega}_1^2 + A_1\omega_1^2 + \frac{B_1}{2}\omega_1^4 = K_1 \tag{4.24}$$

and

$$\dot{\omega}_3^2 + A_3\omega_3^2 + \frac{B_3}{2}\omega_3^4 = K_3, \tag{4.25}$$

where the constants (A_1, B_1, K_1; A_3, B_3, K_3) are given in Table 4.1 and Eq. 4.13. While we anticipated that the phase trajectories defined by Eqs. 4.24 and 4.25 must be closed, they do not necessarily close about the origin. Inspection of the intercepts

$$\dot{\omega}_i \text{ (for } \omega_i = 0) = \pm\sqrt{K_i}$$

$$\omega_i^2 \text{ (for } \dot{\omega}_i = 0) = \frac{-A_i \pm \sqrt{A_i^2 + 2B_iK_i}}{B_i}, \quad i = 1,3 \tag{4.26}$$

immediately reveals that K_1, K_3, $A_1^2 + 2B_1K_1$, and $A_3^2 + 2B_3K_3$ must be all positive for closed trajectories about the origin. It can be shown by substituting from Eqs. 4.13 and Table 4.1 that

$$A_1 + 2B_1K_1 = \left(\frac{(I_2 - I_3)(H^2 - 2I_1T)}{I_1I_2I_3}\right)^2 > 0$$
$$A_3 + 2B_3K_3 = \left(\frac{(I_1 - I_2)(H^2 - 2I_3T)}{I_1I_2I_3}\right)^2 > 0, \tag{4.27}$$

from which it follows that all four ω-intercepts defined by Eq. 4.26 may be real. Inspection of Eqs. 4.13a and 4.13c immediately shows that K_1 and K_3 may be positive or negative; in fact,

$$\text{if} \quad H^2 > 2I_2T, \text{ then } \begin{matrix} K_1 < 0 \\ K_3 > 0 \end{matrix} \tag{4.28}$$

and if

$$H^2 < 2I_2T, \text{ then } \begin{matrix} K_1 > 0 \\ K_3 < 0 \end{matrix} \tag{4.29}$$

It follows that for $H^2 > 2I_2T$ the phase trajectories in ω_1, $\dot{\omega}_1$ space are closed curves not containing the origin (since the $\dot{\omega}$ intercepts are imaginary) while the closed trajectories in ω_3, $\dot{\omega}_3$ space do contain the origin (since both ω and $\dot{\omega}$ intercepts are real). For $H^2 < 2I_2T$ the ω_1, $\dot{\omega}_1$ trajectories contain the origin while ω_3, $\dot{\omega}_3$ trajectories do not. In all cases, the trajectories have mirror symmetry about the ω_i and $\dot{\omega}_i$ axes. The detailed evolution of these phase trajectories is illustrated in an example parametric study (see Figure 4.4 and ref. 4).

The results in Figure 4.4 vividly display the fact that relatively small changes in the behavior of trajectories in one ω, $\dot{\omega}$ plane often correspond to dramatic changes in the other two planes, particularly near the limiting conditions of pure spin about $\hat{\mathbf{b}}_1$, $\hat{\mathbf{b}}_2$, $\hat{\mathbf{b}}_3$. The asymptotic character of pure spin about $\hat{\mathbf{b}}_2$ is clearly displayed in all three planes (case 4). Notice that

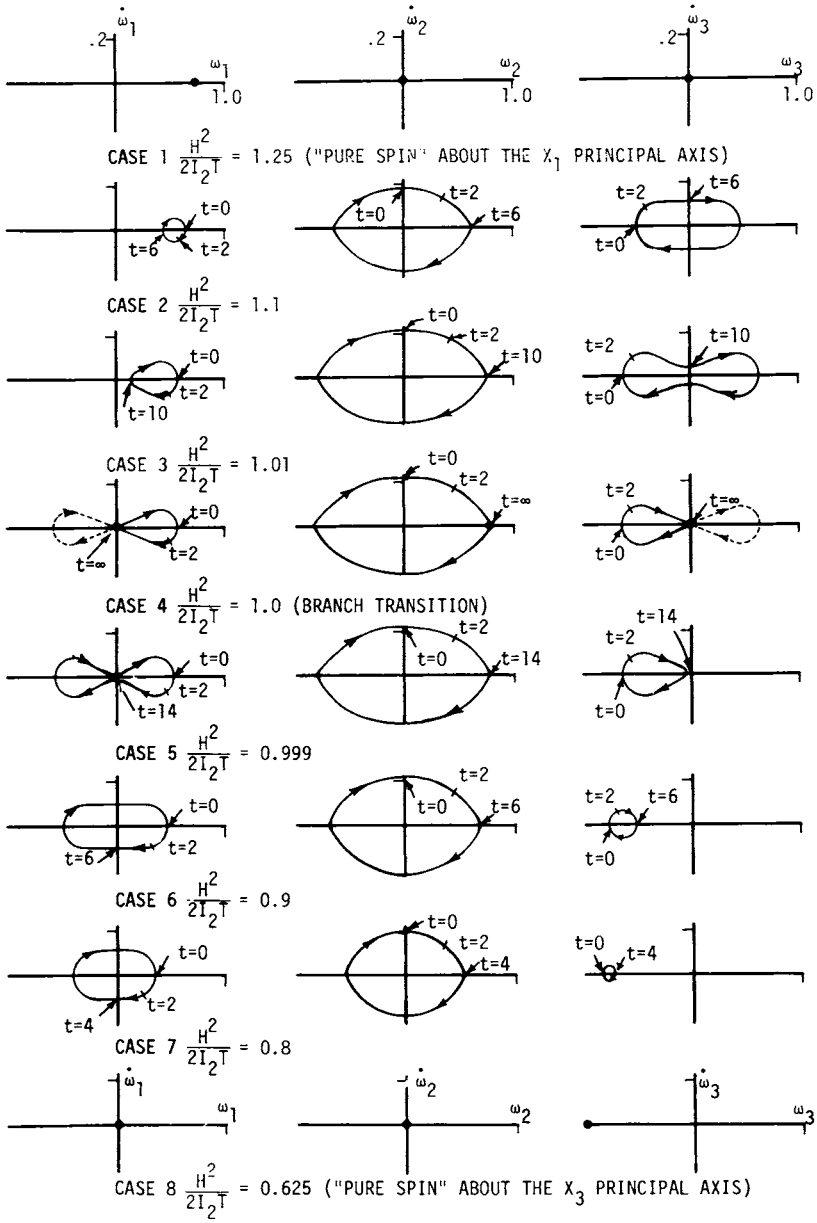

Figure 4.4 A Parametric Study of Rigid Body Dynamics in ω, $\dot{\omega}$ Space

if small angular acceleration disturbances $\{\delta\dot{\omega}_1, \delta\dot{\omega}_2, \delta\dot{\omega}_3\}$ (consistent with $H^2 = 2I_2T$) are imposed upon the motion (initially pure spin about $\hat{b}_2$) then if $\{\delta\dot{\omega}_1 < 0, \delta\dot{\omega}_2 > 0, \delta\dot{\omega}_3 > 0\}$ as time goes to infinity the motion will asymptotically return to pure spin about $\hat{b}_2$. If the $\delta\dot{\omega}$ signs are reversed motion about $\hat{b}_2$ is unstable (in fact pure spin about $-\hat{b}_2$ will ultimately result). Thus, the 'one-sided instability' of permanent rotation about the axis of intermediate inertia is clearly displayed. Similar qualitative observations can easily be made regarding stability of motion near pure spin about the axes of largest and least inertias.

The above results and the related results in Section 4.2.1 are examples of the remarkably rich literature on geometrical constructions and phase portraits associated with torque free motion of a rigid body. We can also construct rigorous motion analogs involving

(i) Ellipsoids rolling without slip on a fixed plane whose normal is the angular momentum vector, the two most famous being due to Poinsot and MacCullagh (refs. 5, 6).

(ii) Elliptical cones rollig without slip on a uniformly rotating plane whose normal is the angular momentum vector. This analogy was also developed by Poinsot, and studied subsequently by Booth (ref. 8), Blanton (ref. 7) and Morton and Junkins (ref. 1).

(iii) For the axi-symmetric special case (two equal principal inertias), a body fixed circular cone rolling without slip on a space-fixed circular cone (ref. 1). The axis of symmetry of the body cone being the body's symmetry axis, while the axis of symmetry of the space cone is the angular momentum vector. The instantaneous angular velocity vector lies along the lines of contact of the two cones.

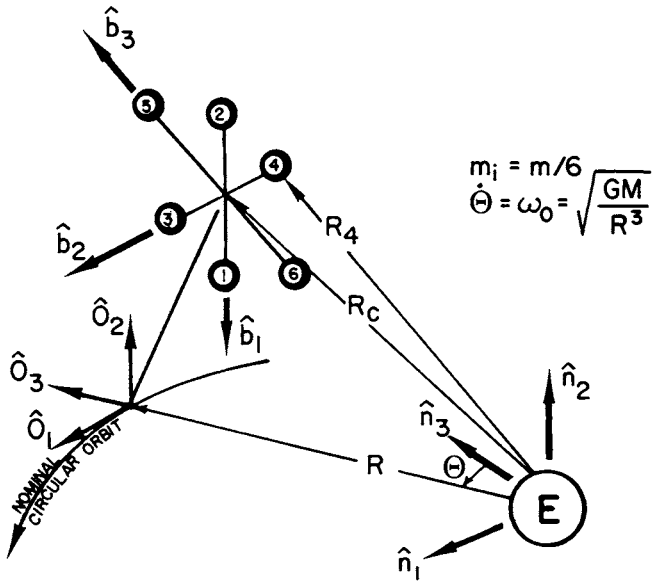

Figure 4.5a A General Displacement of the Rigidly Connected Six Particle Structure

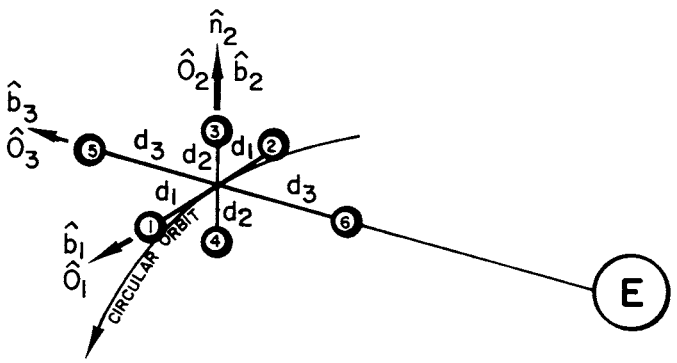

Figure 4.5b The Stable Orientation ($d_3 > d_1 > d_2$, $\hat{b}_3$ is the axis of least inertia, $\hat{b}_2$ is the axis of largest inertia)

Due to the fact that these analogs are well developed in the literature, see for example Morton and Junkins (ref. 1), we elect not to develop the details here. Also, the details of the analytical solution for angular velocity and orientation, given by Morton and Junkins (ref. 1) is not repeated here to avoid the associated treatment of elliptic functions and integrals required for completeness.

4.3 DYNAMICS OF A RIGID SPACE STRUCTURE UNDER THE INFLUENCE OF GRAVITY TORQUES

We now study the case of a finite space structure by considering the motion of the rigid three-axis dumbell configuration shown in Figure 4.5. We are concerned with the attitude dynamics of a large spacecraft in a central inverse square gravity field.

The six point masses are assumed equal to m/6 and to be rigidly connected by three weightless rods of length ($2d_1$, $2d_2$, $2d_3$) as shown. Body fixed principal axes $\{\hat{b}\}$ are angularly displaced from an "orbiting" frame $\{\hat{o}\}$ which has $\hat{o}_3 = R/R$, $\hat{o}_2 = (R \times \dot{R})/|R \times \dot{R}|$, $\hat{o}_1 = \hat{o}_2 \times \hat{o}_3$. For the circular orbit case considered, the orbit frame rotates at a uniform angular velocity $\omega_o = \omega_o \hat{o}_2 = \omega_o \hat{n}_2$, where $\{\hat{n}\}$ are space-fixed axes, and $\omega_o^2 = GM/R^3$ for the nominally circular orbit.

The body $\{\hat{b}\}$ axes are rotationally displaced from the orbit frame $\{\hat{o}\}$ by a direction cosine matrix [C] as

$$\{\hat{b}\} = [C(\psi,\theta,\phi)]\{\hat{o}\} \tag{4.30}$$

which, for 3-2-1 Euler angles, the [C] matrix is

$$[C(\psi,\theta,\phi)] = \begin{bmatrix} 1 & 0 & 0 \\ 0 & c\phi & s\phi \\ 0 & -s\phi & c\phi \end{bmatrix} \cdot \begin{bmatrix} c\theta & 0 & -s\theta \\ 0 & 1 & 0 \\ s\theta & 0 & c\theta \end{bmatrix} \begin{bmatrix} c\psi & s\psi & 0 \\ -s\psi & c\psi & 0 \\ 0 & 0 & 1 \end{bmatrix}$$

or

$$[C(\psi,\theta,\phi)] = \begin{bmatrix} (c\theta c\psi) & (c\theta s\psi) & (-s\theta) \\ (-c\phi s\psi + s\phi\ s\theta c\psi) & (c\phi c\psi + s\phi\ s\theta\ s\psi) & (s\phi c\theta) \\ (s\phi s\psi + c\phi\ s\theta c\psi) & (-s\phi c\psi + c\phi s\theta s\psi) & (c\phi c\theta) \end{bmatrix} \quad (4.31)$$

where $c \equiv \cos$, $s \equiv \sin$. The angular velocity ω of body axes $\{\hat{b}\}$ with respect to the inertial frame $\{\hat{n}\}$ is

$$\omega = (\Omega_1\hat{b}_1 + \Omega_2\hat{b}_2 + \Omega_3\hat{b}_3) + \omega_o\hat{o}_2 \quad (4.32)$$

where the parenthetic expression is the angular velocity of $\{\hat{b}\}$ relative to the uniformly rotating orbit $\{\hat{o}\}$ frame; from Table 2.1, the Ω_i are related to the angular rates by the kinematic equations

$$\begin{aligned} \Omega_1 &= \dot{\phi} - \dot{\psi}\sin\theta \\ \Omega_2 &= \dot{\theta}\cos\phi + \dot{\psi}\cos\theta\sin\phi \\ \Omega_3 &= -\dot{\theta}\sin\phi + \dot{\psi}\cos\theta\cos\phi \end{aligned} \quad (4.33)$$

Since, from Eqs. 4.30 and 4.31,

$$\begin{aligned} \hat{o}_2 = {} & (\cos\theta\sin\psi)\hat{b}_1 + (\cos\phi\cos\psi + \sin\phi\sin\theta\sin\psi)\hat{b}_2 \\ & + (-\sin\phi\cos\psi + \cos\phi\sin\theta\sin\psi)\hat{b}_3 \end{aligned} \quad (4.34)$$

then the $\{\hat{b}\}$ components of $\{\hat{b}\}$'s inertial angular velocity $\omega = \omega_1\hat{b}_1 + \omega_2\hat{b}_2 + \omega_3\hat{b}_3$ are obtained by substituting Eq. 4.33 and Eq. 4.34 into Eq. 4.32 as

$$\begin{aligned} \omega_1 &= \dot{\phi} - \dot{\psi}\sin\theta + \omega_o(\cos\theta\sin\psi) \\ \omega_2 &= \dot{\theta}\cos\phi + \dot{\psi}\cos\theta\sin\phi + \omega_o(\cos\phi\cos\psi + \sin\phi\sin\theta\sin\psi) \\ \omega_3 &= -\dot{\theta}\sin\phi + \dot{\psi}\cos\theta\cos\phi + \omega_o(-\sin\phi\cos\psi + \cos\phi\sin\theta\sin\psi) \end{aligned} \quad (4.35)$$

It is apparent, by inspection of Figure 4.5 that the inertia matrix for the dumbell configuration (about the mass center, with respect to the $\{\hat{b}\}$ axes, ignoring mass of the connecting booms) is

$$I = \frac{m}{3}\begin{bmatrix} (d_2^2 + d_3^2) & 0 & 0 \\ 0 & (d_1^2 + d_3^2) & 0 \\ 0 & 0 & (d_1^2 + d_2^2) \end{bmatrix} \equiv \begin{bmatrix} I_1 & 0 & 0 \\ 0 & I_2 & 0 \\ 0 & 0 & I_3 \end{bmatrix} \quad (4.36)$$

m = total mass (each of the equal masses is $m/6$).

Notice, the vectors locating the six masses (relative to the nonrotating $\{\hat{n}\}$

frame with an origin at the earth's mass center) are

$$\mathbf{R}_i = \mathbf{R} + \mathbf{r} + \Delta\mathbf{r}_i \quad , \quad i = 1,2,\ldots,6 \tag{4.37}$$

where

$$\mathbf{r} = x\,\hat{o}_1 + y\,\hat{o}_2 + z\,\hat{o}_3 \tag{4.38}$$

and

$$\begin{aligned} \Delta\mathbf{r}_1 &= d_1\,\hat{b}_1 \ , \ \Delta\mathbf{r}_2 = -d_1\,\hat{b}_1 \\ \Delta\mathbf{r}_3 &= d_2\,\hat{b}_2 \ , \ \Delta\mathbf{r}_4 = -d_2\,\hat{b}_2 \\ \Delta\mathbf{r}_5 &= d_3\,\hat{b}_3 \ , \ \Delta\mathbf{r}_6 = -d_3\,\hat{b}_3 \end{aligned} \tag{4.39}$$

We note in passing, lest the developments seem like a not-too-exciting special case, that the six mass dumbell is "inertially equivalent" to a general rigid body of mass m; the masses are uniquely positioned as a function of m and the body's arbitrary inertias (I_1, I_2, I_3) according to

$$\begin{aligned} d_1 &= \sqrt{\frac{3}{2m}\,\alpha} \ , \ \alpha = -I_1 + I_2 + I_3 \\ d_2 &= \sqrt{\frac{3}{2m}\,\beta} \ , \ \beta = I_1 - I_2 + I_3 \\ d_3 &= \sqrt{\frac{3}{2m}\,\gamma} \ , \ \gamma = I_1 + I_2 - I_3 \end{aligned} \tag{4.40}$$

Since (α,β,γ) are non negative (for all physically admissible inertia values), it follows that real values for the d_i always exist. Thus, the dumbell is a configuration used for conceptual symplicity, but the results obtained hold for a general rigid body.

The gravitational force on the i^{th} mass is

$$\mathbf{F}_i = -\frac{GMm_i}{R_i^3}\,\mathbf{R}_i \quad , \quad i = 1,2,\ldots,6 \quad , \quad m_i = m/6 \tag{4.41}$$

To further simplify the initial discussion, let us constrain the mass center to move along the nominal circular orbit. This permits us to set $\mathbf{r} = 0$ (see Figure 4.5a) and ignores a weak rotational/translational coupling, but retains the translational/rotational coupling (gravity torque as a function of orbital position) to a high approximation. The validity and effects of this assumption

will subsequently be studied. Thus we take

$$\mathbf{R}_i = \mathbf{R} + \Delta\mathbf{r}_i \quad , \quad i = 1,2,\ldots,6 \tag{4.42}$$

and

$$R_i^2 = (\mathbf{R} + \Delta\mathbf{r}_i) \cdot (\mathbf{R} + \Delta\mathbf{r}_i) = R^2(1 + \alpha_i) \quad , \quad i = 1,2,\ldots,6 \tag{4.43}$$

with

$$\alpha_i = \frac{1}{R^2}(2\mathbf{R} \cdot \Delta\mathbf{r}_i + \Delta\mathbf{r}_i \cdot \Delta\mathbf{r}_i) \tag{4.44}$$

Since $R_i^{-3} = (R_i^2)^{-3/2}$, we use the binomial expansion to write

$$\frac{1}{R_i^3} = \frac{1}{R^3}(1 - \frac{3}{2}\alpha_i + \ldots) \tag{4.45}$$

so that

$$\begin{aligned}
&\frac{1}{R_1^3} \cong \frac{1}{R^3}(1\text{-}3\,C_{13}\frac{d_1}{R}) \quad , \quad \frac{1}{R_2^3} \cong \frac{1}{R^3}(1\text{+}3\,C_{13}\frac{d_1}{R}) \\
&\frac{1}{R_3^3} \cong \frac{1}{R^3}(1\text{-}3\,C_{23}\frac{d_2}{R}) \quad , \quad \frac{1}{R_4^3} \cong \frac{1}{R^3}(1\text{+}3\,C_{23}\frac{d_2}{R}) \\
&\frac{1}{R_5^3} \cong \frac{1}{R^3}(1\text{-}3\,C_{33}\frac{d_3}{R}) \quad , \quad \frac{1}{R_6^3} \cong \frac{1}{R^3}(1\text{+}3\,C_{33}\frac{d_3}{R})
\end{aligned} \tag{4.46}$$

where we also made use of

$$\mathbf{R} = R\,\hat{\mathbf{o}}_3 = R(C_{13}\,\hat{\mathbf{b}}_1 + C_{23}\,\hat{\mathbf{b}}_2 + C_{33}\,\hat{\mathbf{b}}_3) \tag{4.47}$$

and Eq. 4.39 for $\Delta\mathbf{r}_i$.

Note, if we calculate the net external (gravitational) force

$$\mathbf{F} = \sum_{i=1}^{6} \mathbf{F}_i \tag{4.48}$$

we find

$$\begin{aligned}
\mathbf{F} = \frac{-GMm}{6R^3}\{&(1\text{-}3C_{13}\frac{d_1}{R})(\mathbf{R} + d_1\,\hat{\mathbf{b}}_1) + (1\text{+}3\,C_{13}\frac{d_1}{R})(\mathbf{R} - d_1\,\hat{\mathbf{b}}_1) \\
&+(1\text{-}3C_{23}\frac{d_2}{R})(\mathbf{R} + d_2\,\hat{\mathbf{b}}_2) + (1\text{+}3\,C_{23}\frac{d_2}{R})(\mathbf{R} - d_2\,\hat{\mathbf{b}}_2) \\
&+(1\text{-}3C_{33}\frac{d_3}{R})(\mathbf{R} + d_3\,\hat{\mathbf{b}}_3) + (1\text{+}3\,C_{33}\frac{d_3}{R})(\mathbf{R} - d_3\,\hat{\mathbf{b}}_3)\} + \ldots
\end{aligned}$$

or

$$F = \frac{-GM(m)}{R^3} R - \frac{GM(m)}{R^4} (d_1^2 C_{13} \hat{b}_1 + d_2^2 C_{23} \hat{b}_2 + d_3^2 C_{33} \hat{b}_3) + \ldots \quad (4.49)$$

Since the first term is precisely the force on a particle of mass m moving along the nominal circular orbit, we can interpret the second term as the "constraint force" required to maintain the circular translational motion in the presence of coupling with rotational dynamics, and accounting for the finite size of the structure.

Let us introduce the circular orbit frequency $\omega_o^2 = GM/R^3$ so that Eq. 4.49 becomes

$$F = -mR\omega_o^2 [(1)\hat{o}_3 + (\frac{d_1}{R})^2 C_{13} \hat{b}_1 + (\frac{d_2}{R})^2 C_{23} \hat{b}_2 + (\frac{d_3}{R})^2 C_{33} \hat{b}_3] \quad (4.50)$$

It is evident from Eq. 4.50 (for typical spacecraft configurations with $d_i \approx 10m$, $R \cong 7 \times 10^6$ m, $(d_i/R)^2 \cong 10^{-10}$) that ignoring the attitude to orbit coupling is typically valid to one part in 10^{10}; thus, even for larger spacecraft, it is an altogether reasonable first approximation to ignore the rotational-to-translational coupling effects. The translational-to-rotational coupling terms, however, while small, are usually *not negligible*. The translation-induced $(\frac{1}{R^2})$ variations in intensity of the gravity field along an elliptic orbit cause significant, non-negligible gravity torque variations. We restrict our detailed discussion to the circular orbit case.

Let us now consider the rotational dynamics. We begin by finding compact expressions for the torque acting on the configuration of Figure 4.5. By definition, the torque about the mass center is determined by summing the moments generated by the external forces F_i as

$$L_c = \sum_{i=1}^{6} \Delta r_i \times F_i \quad (4.51)$$

Substituting Eqs. 4.39, 4.41, 4.46, and 4.47 into Eq. 4.51 leads directly to

$$L_c = \frac{GMm}{R^3}\{d_1^2\, C_{13}(\hat{b}_1 \times \hat{o}_3) + d_2^2\, C_{23}(\hat{b}_2 \times \hat{o}_3) + d_3^2\, C_{33}(\hat{b}_3 \times \hat{o}_3)\} \tag{4.52}$$

Substituting $\hat{o}_3 = C_{13}\,\hat{b}_1 + C_{23}\,\hat{b}_2 + C_{33}\,\hat{b}_3$ reduces Eq. 4.52 to

$$L_c = \frac{GMm}{R^3}\{(d_2^2-d_3^2)C_{23}\,C_{33}\,\hat{b}_1 + (d_3^2-d_1^2)C_{13}\,C_{33}\,\hat{b}_2 + (d_1^2-d_2^2)C_{13}\,C_{23}\,\hat{b}_3\}$$

and, making use of

$$\begin{aligned} I_1 - I_2 &= \tfrac{1}{3}\, m\, (d_2^2 - d_1^2) \\ I_1 - I_3 &= \tfrac{1}{3}\, m\, (d_3^2 - d_1^2) \\ I_2 - I_3 &= \tfrac{1}{3}\, m\, (d_3^2 - d_2^2) \end{aligned} \tag{4.53}$$

We find

$$L_c = L_1\,\hat{b}_1 + L_2\,\hat{b}_2 + L_3\,\hat{b}_3 \tag{4.54}$$

with the body axis gravitational "gravity gradient" torque components

$$\begin{aligned} L_1 &= 3\,\frac{GM}{R^3}\,(I_3 - I_2)C_{23}\,C_{33} \\ L_2 &= 3\,\frac{GM}{R^3}\,(I_1 - I_3)C_{13}\,C_{33} \\ L_3 &= 3\,\frac{GM}{R^3}\,(I_2 - I_1)C_{13}\,C_{23} \end{aligned} \tag{4.55}$$

We digress briefly to point out that a more general development leads to the identical torque expressions. For an arbitrary continuous mass distribution, the torque is determined by integrating the differential torques over the body(S) as

$$L_c = \iiint_S \Delta\mathbf{r} \times d\mathbf{F} = \iiint_S \Delta\mathbf{r} \times \left(-\frac{GM}{r^3}\,\mathbf{r}\right)dm$$

where, we find that substituting

$$\Delta\mathbf{r} = x_1\,\hat{b}_1 + x_2\,\hat{b}_2 + x_3\,\hat{b}_3$$

$$\mathbf{r} = R\,\hat{o}_3 + \Delta\mathbf{r}$$

$$\hat{o}_3 = C_{13}\,\hat{b}_1 + C_{23}\,\hat{b}_2 + C_{33}\,\hat{b}_3$$

$$\frac{1}{r^3} = \frac{1}{R^3}\left\{1 + 3\left[C_{13}\left(\frac{x_1}{R}\right) + C_{23}\left(\frac{x_2}{R}\right) + C_{33}\left(\frac{x_3}{R}\right)\right] + \ldots\right\}$$

leads immediately to the general gravity gradient torque

$$\begin{aligned} \underline{L}_c = \frac{3GM}{R^3} \{ & [C_{23}C_{33}(I_{33} - I_{22}) - C_{13}C_{33}I_{12} + C_{13}C_{23}I_{13} - (C_{33}^2 - C_{23}^2)I_{23}]\hat{\underline{b}}_1 \\ & + [C_{13}C_{33}(I_{11} - I_{33}) - C_{13}C_{23}I_{23} + C_{33}C_{23}I_{12} - (C_{13}^2 - C_{33}^2)I_{13}]\hat{\underline{b}}_2 \\ & + [C_{13}C_{23}(I_{22} - I_{11}) - C_{23}C_{33}I_{13} + C_{13}C_{33}I_{23} - (C_{23}^2 - C_{13}^2)I_{12}]\hat{\underline{b}}_3 \} \\ & + \ldots \end{aligned} \tag{4.56}$$

where we made use of

$$\iiint_S x_i dm = 0 \quad , \quad i = 1,2,3. \tag{4.57}$$

as a consequence of the fact that the origin is the mass center of the configuration, and we used the usual definitions of the inertias introduced in Eq. 3.22. Obviously, for the case that $\{\hat{\underline{b}}\}$ is chosen as principal axes, the products of inertia terms vanish and Eq. 4.56a reduces immediately to Eq. 4.55. Once again, we point out that the results obtained for the dumbell configuration are quite general, owing to the inertial equivanence of the dumbell to a general rigid body.

The torque components Eq. 4.56 can be written in terms of the yaw, pitch, roll, and Euler angles (ψ,θ,ϕ), by substituting the C_{ij} from Eq. 4.31, and substituting $\omega_o^2 = GM/R^3$. The resulting torque expressions are

$$\begin{aligned} L_1 &= \frac{3}{2}\omega_o^2 (I_3 - I_2)\cos^2\theta \sin 2\phi \\ L_2 &= -\frac{3}{2}\omega_o^2(I_1 - I_3)\cos\phi \sin 2\theta \\ L_3 &= -\frac{3}{2}\omega_o^2(I_2 - I_1)\sin\phi \sin 2\theta \end{aligned} \tag{4.58}$$

Prior to development of the rotational equations of motion, analysis of the above torque expressions provides some direct insight. First, let us note the conditions under which all three torques in Eq. 4.58 simultaneously vanish:

I. $I_1 = I_2 = I_3$

II. $\phi = \theta = 0, \pi$

III. $\phi = \pm \pi/2, \theta = \pm \pi/2$

We conclude from possibility I that a spherically symmetric spacecraft does not have a preferred gravitational orientation. From possibilities II and III, we find that aligning any one of the principal axes with the radius vector $\mathbf{R} = R\,\hat{o}_3$ causes the gravity torque to vanish. Since the labeling of the axes is arbitrary, we see that this statement includes both the "up" and "down" pointing of each principal axis. Notice, *the gravitational torque does not depend upon the ψ (yaw) rotation about $\hat{o}_3$.* We will subsequently find, however, that there is a preferred yaw orientation (we'll find $\hat{b}_2 \equiv \pm \hat{o}_2$ is usually the stable orientation, if $\hat{b}_2$ is the axis of largest inertia and if energy dissipation effects are taken into account); but it is evident from Eq. 4.58, that a pure yaw rotation is immaterial vis-a-vis variations in the gravity gradient torque acting on a rigid body. Using energy sink arguments, we can anticipate that the preferred orientation is alignment of the maximum axis of inertia with the angular momentum vector ($\hat{b}_2 = \hat{o}_2 = \hat{n}_2$). It is important to remind ourselves that the present discussion is concerned only with motion under the assumptions of an inverse square gravity field, a rigid spacecraft model, and a circular orbit.

Since labeling of axes is arbitrary, analysis of small oscillations near $(\phi,\theta) = (0,0)$ (leaving $I_1 \gtrless I_2 \gtrless I_3 \gtrless I_1$ unspecified) will yield all the cases for which one of the principal axes is nearly aligned with the local vertical $\hat{o}_3$.

In particular, if we assume ϕ and θ to be small angles, note that the torque Eq. 4.58 linearizes to

$$L_1 \cong -3\omega_o^2(I_2 - I_3)\phi$$

$$L_2 \cong -3\omega_o^2(I_1 - I_3)\theta$$

$$L_3 \cong 0 \tag{4.59}$$

From which we conclude that the roll (L_1) and pitch (L_2) torques are "restoring" only if

$$I_2 \geq I_3 \text{ and } I_1 \geq I_3 \tag{4.60}$$

The conditions of Eq. 4.60 require that $\hat{b}_3$ be the axis of least inertia (and, be nearly aligned with $\hat{o}_3$).

Let us now derive the differential equations for small angular motion near the condition ($\phi = \theta = \psi = 0$). For small angles and angular rates, the kinematic Eq. 4.35 linearize to provide

$$\begin{aligned} \omega_1 &\cong \dot{\phi} + \omega_o \psi \\ \omega_2 &\cong \dot{\theta} + \omega_o \\ \omega_3 &\cong \dot{\psi} - \omega_o \phi \end{aligned} \tag{4.61}$$

Substitution of Eqs. 4.61 and 4.59 into the Euler equation of Eq. 3.31

$$\begin{aligned} L_1 &= I_1 \dot{\omega}_1 + (I_3 - I_2)\omega_2 \omega_3 \\ L_2 &= I_2 \dot{\omega}_2 + (I_1 - I_3)\omega_1 \omega_3 \\ L_3 &= I_3 \dot{\omega}_3 + (I_2 - I_1)\omega_1 \omega_2 \end{aligned} \tag{4.62}$$

immediately yields

$$\begin{aligned} \textit{roll:} \quad & 3\omega_o^2(I_3 - I_2)\phi = I_1(\ddot{\phi} + \omega_o\dot{\psi}) + (I_3 - I_2)(\dot{\theta} + \omega_o)(\dot{\psi} - \omega_o\phi) \\ \textit{pitch:} \quad & -3\omega_o^2(I_1 - I_3)\theta = I_2\ddot{\theta} + (I_1 - I_3)(\dot{\phi} + \omega_o\psi)(\dot{\psi} - \omega_o\phi) \\ \textit{yaw:} \quad & 0 = I_3(\ddot{\psi} - \omega_o\dot{\phi}) + (I_2 - I_1)(\dot{\phi} + \omega_o\psi)(\dot{\theta} + \omega_o) \end{aligned}$$

which simplify to provide three second-order, linear differential equations:

$$\textit{pitch:} \qquad \ddot{\theta} = -\Omega^2\theta \;, \quad \Omega^2 = 3\left(\frac{I_1 - I_3}{I_2}\right)\omega_o^2 \tag{4.63}$$

$$\textit{roll/yaw:} \begin{bmatrix} I_1 & 0 \\ 0 & I_3 \end{bmatrix} \begin{Bmatrix} \ddot{\phi} \\ \ddot{\psi} \end{Bmatrix} = -\begin{bmatrix} 4\omega_o^2(I_2 - I_3) & 0 \\ 0 & (I_2 - I_1)\omega_o^2 \end{bmatrix} \begin{Bmatrix} \phi \\ \psi \end{Bmatrix} + \begin{bmatrix} 0 & -\omega_o\beta \\ \omega_o\beta & 0 \end{bmatrix} \begin{Bmatrix} \dot{\phi} \\ \dot{\psi} \end{Bmatrix} \tag{4.64}$$

where we made use of $\beta \equiv I_1 - I_2 + I_3$ from Eq. 4.42. Notice, to first-order, that the pitch motion uncouples in Eq. 4.63 and the motion is divergent unless $\Omega^2 \geq 0$; this immediately yields the pitch stability requirement

$$I_1 \geq I_3 \tag{4.65}$$

Roll/yaw stability is governed by the eigenvalues of the *gyroscopic* differential equation Eq. 4.64. The discussion can be put in standard form by introducing the roll/yaw state vector

$$X \equiv (\phi \ \psi \ \dot{\phi} \ \dot{\psi})^T \tag{4.66}$$

and rewriting Eq. 4.64 in the first-order form

$$\dot{X} = F\,X \tag{4.67}$$

with the coefficient matrix

$$F = \begin{bmatrix} 0 & 0 & 1 & 0 \\ 0 & 0 & 0 & 1 \\ -4\omega_o^2\left(\frac{I_2-I_3}{I_1}\right) & 0 & 0 & \frac{-\omega_o\beta}{I_1} \\ 0 & -\omega_o^2\left(\frac{I_2-I_1}{I_3}\right) & \frac{\omega_o\beta}{I_3} & 0 \end{bmatrix} \tag{4.68}$$

The eigenvalues of F are the roots of the characteristic equation

$$c(\lambda) = \det\,(F - \lambda I) = \lambda^4 + \alpha_1 \lambda^2 + \alpha_2 = 0 \tag{4.69}$$

with

$$\alpha_1 = \frac{\omega_o^2}{I_1 I_3}\left[\beta^2 + I_1(I_2 - I_1) + 4I_3(I_2 - I_3)\right] \tag{4.70a}$$

$$\alpha_2 = \frac{4\omega_o^2}{I_1 I_3}(I_2 - I_3)(I_2 - I_1) \tag{4.70b}$$

For non-divergent motion, it is necessary and sufficient that none of the four eigenvalues (roots of Eq. 4.69) have positive real parts. By explicitly solving for these roots or applying the Routh-Hurwitz Criterion, (ref. 5) we

find that requiring all four roots to have non-positive real parts dictates the sufficient conditions

$$\alpha_1 \geq 0 \tag{4.71a}$$

$$\alpha_2 \geq 0 \tag{4.71b}$$

$$\alpha_1^2 - 4\alpha_2 \geq 0 \tag{4.71c}$$

in which case the four eigenvalues are purely imaginary. Imposing Eq. 4.71b on Eq. 4.70b leads to two possibilities

(i) $I_2 \geq I_3$ and $I_2 \geq I_1$

or

(ii) $I_2 \leq I_3$ and $I_2 \leq I_1$

By inspection, we see that possibility (i) causes Eq. 4.70a to satisfy Eq. 4.71a for all possible inertias. Possibility (ii), however is not consistent with the conditions of Eq. 4.60; therefore, we can reject it on physical grounds. The inclusion of a damping model usually results in case (i) being stable and case (ii) unstable. Thus, condition (i) together with the pitch stability requirement of Eq. 4.65 allows us to summarize sufficient conditions for neutral stability (nondivergent oscillations or "liberations") as

$$I_2 \geq I_1 \geq I_3 \tag{4.72}$$

By varying the inertias in Eqs. 4.70, detailed study of the roots of Eq. 4.69 allow us to construct the regions of stability as shown in Fig. 4.6. The small third quadrant stable region is not utilized in practice beacuse it's shape (and stability margin) is very sensitive to modeling errors and the presence of dampers. The stable orientation is shown in Figure 4.5b. The axis of least inertia is aligned with the local vertical; the axis of largest inertia is the once-per-orbit "spin" axis aligned with the orbit normal. One can show that this latter state is a minimum energy state. We note in passing that our moon is a prominent natural example of a gravity gradient stabilized satellite.

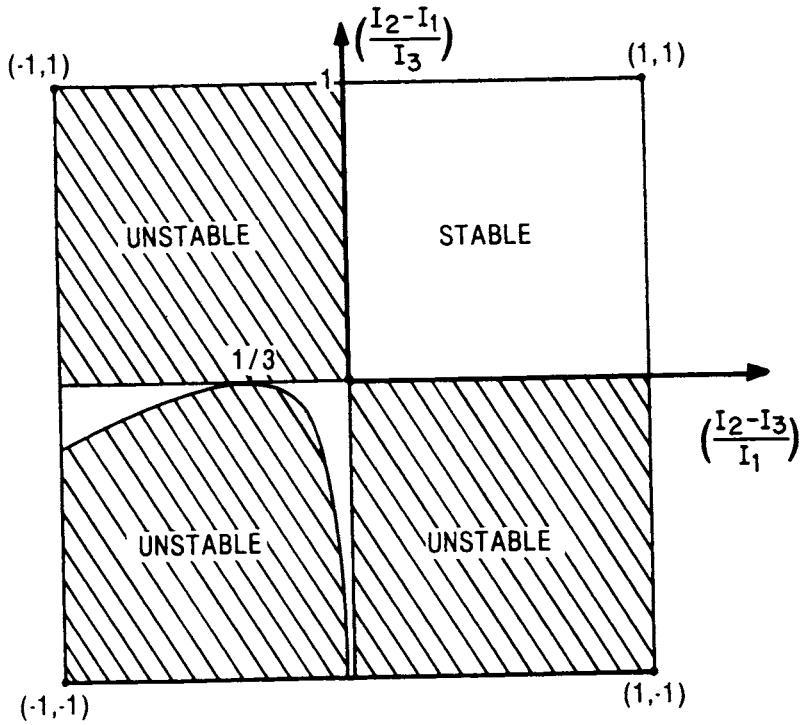

Figure 4.6 Stable Versus Unstable Inertia Ratios for Gravity Gradient Stabilized Spacecraft

We now briefly consider the solution of the translational/rotational dynamic equations of motion *without* imposing the constraint that the mass center move along a circular orbit. The system total energy is

$$E = T + V \tag{4.73}$$

where

$$T = \frac{1}{2}\left(\sum_{i=1}^{6} m_i\right)\dot{R}_c \cdot \dot{R}_c + \frac{1}{2}\left(I_1\omega_1^2 + I_2\omega_2^2 + I_3\omega_3^2\right) \tag{4.74}$$

$$V = -\sum_{i=1}^{6} GMm_i/R_i \quad , \quad m_i = m/6 \tag{4.75}$$

$$\dot{R}_c = [\dot{x} + (R + z)\omega_o]\hat{o}_1 + \dot{y}\hat{o}_2 + [\dot{z} - x\omega_o]\hat{o}_3 \tag{4.76}$$

$$\frac{1}{R_i} = \frac{1}{R}\frac{1}{\sqrt{1+\alpha_i}} \quad , \quad i = 1,2,\ldots,6 \tag{4.77}$$

$$\begin{aligned}
R^2\alpha_1 &= x^2 + y^2 + z^2 + d_1^2 + 2\,d_1(x\,C_{11} + y\,C_{12} + z\,C_{13}) + 2R(z + d_1C_{13}) \\
R^2\alpha_2 &= x^2 + y^2 + z^2 + d_1^2 - 2\,d_1(x\,C_{11} + y\,C_{12} + z\,C_{13}) + 2R(z - d_1C_{13}) \\
R^2\alpha_3 &= x^2 + y^2 + z^2 + d_2^2 + 2\,d_2(x\,C_{21} + y\,C_{22} + z\,C_{23}) + 2R(z + d_2C_{23}) \\
R^2\alpha_4 &= x^2 + y^2 + z^2 + d_2^2 - 2\,d_2(x\,C_{21} + y\,C_{22} + z\,C_{23}) + 2R(z - d_2C_{23}) \\
R^2\alpha_5 &= x^2 + y^2 + z^2 + d_3^2 + 2\,d_3(x\,C_{31} + y\,C_{32} + z\,C_{33}) + 2R(z + d_3C_{33}) \\
R^2\alpha_6 &= x^2 + y^2 + z^2 + d_3^2 - 2\,d_3(x\,C_{31} + y\,C_{32} + z\,C_{33}) + 2R(z - d_3C_{33})
\end{aligned} \tag{4.78}$$

Upon substituting into Eq. 4.73, the constant total energy can be found to have the form

$$E = E_o + E_1 + E_2 \tag{4.79}$$

where

$E_o = mR^2\omega_o^2/2 + I_2\omega_o^2/2 + \text{const}$, the nominal energy of the reference motion" state. (4.80)

E_1 is a linear function of the coordinates and velocities.

E_2 is a quadratic function of the coordinates and velocities, plus all higher order terms.

It is a lengthy algebraic exercise, but it can be established that the total potential energy expression obtained for Eq. 4.75 achieves a minimum at the

point $(x,y,z,\psi,\theta,\phi) = 0$; this minimum energy state corresponds to the case that the $\hat{b}_2$ is the axis of largest inertia, aligned with the orbit normal, as shown in Figure 4.5b.

Having considered small motions of an orbiting rigid body subject to gravity gradient torques, we now seek to generalize these results to consider non-rigid bodies and collections of bodies.

4.4 DYNAMICS OF MULTI-WHEEL CONFIGURATIONS

The attitude control and stabilization systems of many modern spacecraft (ref. 9) involve one or more rotors and associated electric motors to generate torques about the rotor spin axis. A rotor (spinning about a spacecraft-fixed axis) has two traditional qualitative uses:

(i) To store a "bias" angular momentum to render the attitude motion stiff with respect to rotations about axes perpendicular to the rotor (momentum wheel) spin axis. We can, in fact, stabilize an otherwise rigid spacecraft about any of its principal axes by using an appropriate momentum bias.

(ii) To use as a reaction device for generating attitude control torques. Upon applying (via an electric motor) a torque to the rotor, an equal and opposite torque is applied to the spacecraft.

The above uses must be based upon a carefully formulated mathematical model of the system. Primarily due to gyroscopic effects, as is evident in the foregoing paragraphs (Sections 4.2 - 4.3), a single rigid body displays a variety of nonlinear gyroscopic motions, so it is not surprising that coupled rigid bodies exhibit a rich variety of nontrivial, nonlinear motions due to the competing, coupled gyroscopic effects. We consider here a sequence of dynamical systems having increasing degrees of generality in the number, location and orientation of the rotors imbedded in a general rigid body.

4.4.1 Dual Spin Configuration

With reference to Figure 4.7, we consider a general rigid body having a symmetric rotor whose axis of symmetry is aligned with one of its three principal axes of the coupled two body system. Notice, since rotation of the symmetric rotor does not redistribute mass, the principal axes are invariant with respect to the rotor motion. We neglect the displacement of the rotor from the system mass center. We ignore translational motion of the system and are concerned initially only with the rotational dynamics.

The system angular momentum is

$$\mathbf{H} = \mathbf{H}_B + \mathbf{H}_W \tag{4.81}$$

where the body B angular momentum vector has the B-fixed $\{\hat{\mathbf{b}}\}$ components

$$\mathbf{H}_B = I_1^* \omega_1 \hat{\mathbf{b}}_1 + I_2^* \omega_2 \hat{\mathbf{b}}_2 + I_3^* \omega_3 \hat{\mathbf{b}}_3 \tag{4.82}$$

and the rotor (wheel, W) angular momentum vector has the B-fixed components

$$\mathbf{H}_W = J_1 \omega_1 \hat{\mathbf{b}}_1 + J_2 (\omega_2 + \Omega)\hat{\mathbf{b}}_2 + J_3 \omega_3 \hat{\mathbf{b}}_3 \tag{4.83}$$

and

(I_1^*, I_2^*, I_3^*) are the principal inertias of B.

$(J_1, J_2, J_3 = J_1)$ are the principal inertias of W.

$(\omega_1, \omega_2, \omega_3)$ are the $\{\hat{\mathbf{b}}\}$ components of B's inertial angular velocity

Ω is the angular speed of W to B, positive in right hand sense about $\hat{\mathbf{b}}_2$.

Substitution of Eqs. 4.82 and 4.83 into Eq. 4.81 yields

$$\mathbf{H} = H_1 \hat{\mathbf{b}}_1 + H_2 \hat{\mathbf{b}}_2 + H_3 \hat{\mathbf{b}}_3. \tag{4.84}$$

with

$$H_1 = I_1 \omega_1 \tag{4.85a}$$

$$H_2 = I_2 \omega_2 + h_2 \tag{4.85b}$$

$$H_3 = I_3 \omega_3 \tag{4.85c}$$

and

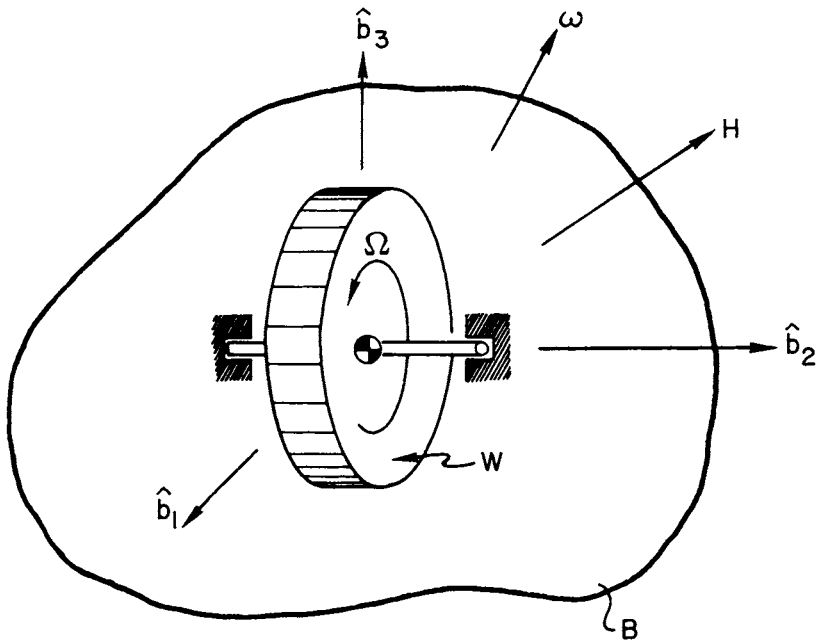

Figure 4.7 A Dual Spin Configuration

$I_i = I_i^* + J_i$, i = 1,2,3, the 2-body system's principal inertias. (4.86)

$h_2 = J_2\,\Omega$, the relative momentum. (4.87)

The system rotational equations of motion follow from Euler's equation

$$L = \dot{H} = \frac{d}{dt}(H)_N = \frac{d}{dt}(H)_B + \omega \times H \tag{4.88}$$

Substitution of Eqs. 4.84 and 4.85 into Eq. 4.88 yields the spacecraft equations of motion:

Roll: $L_1 = I_1\,\dot{\omega}_1 + (I_3 - I_2)\omega_2\,\omega_3 - \omega_3\,h_2$ (4.89a)

Pitch: $L_2 = I_2\,\dot{\omega}_2 + (I_1 - I_3)\omega_3\,\omega_1 + \dot{h}_2$ (4.89b)

Yaw: $L_3 = I_3\,\dot{\omega}_3 + (I_2 - I_1)\omega_1\,\omega_2 + \omega_1 h_2$ (4.89c)

The internal degree of freedom can be obtained in several ways. The simplest is to simply set the motor torque $u(t)\,\hat{b}_2$ applied to W (note, $-u(t)\,\hat{b}_2$ is applied to B) equal to the time derivative of the $\hat{b}_2$ component of W's angular momentum. Thus we obtain

Wheel dynamics: $u(t) = J_2(\dot{\omega}_2 + \dot{\Omega}) = J_2\,\dot{\omega}_2 + \dot{h}_2$ (4.90)

Upon eliminating $\dot{h}_2$, by substituting Eq. 4.90 into Eq. 4.89b, we obtain a modified pitch equation

Pitch: $L_2 = I_2^*\,\dot{\omega}_2 + (I_1 - I_3)\omega_3\,\omega_1 + u(t)$ (4.91)

and, finally, the wheel's equation of motion (4.90) becomes, upon substituting for $\dot{\omega}_2$ from Eq. 4.91.

Wheel dynamics: $\dot{h}_2 = \left(\frac{J_2}{I_2^*}\right)(I_1 - I_3)\omega_3\,\omega_1 - \left(\frac{J_2}{I_2^*}\right)L_2 + \left(\frac{I_2}{I_2^*}\right)u$ (4.92)

Observe the system's total energy is

$$E = \frac{1}{2}\,[I_1^*\,\omega_1^2 + I_2^*\,\omega_2^2 + I_3^*\,\omega_3^2] + \frac{1}{2}\,[J_1\,\omega_1^2 + J_2\,(\omega_2 + \Omega)^2 + J_1\,\omega_3^2] \tag{4.93}$$

or

$$E = \frac{1}{2}\,(I_1\,\omega_1^2 + I_2\,\omega_2^2 + I_3\,\omega_3^2) + \frac{1}{2}\,\frac{1}{J_2}\,h_2^2 + \omega_2\,h_2 \tag{4.94}$$

It is easy to verify (by differentiation of Eq. 4.94 and substitution for $\dot{\omega}_i$ and $\dot{h}_2$ from Eqs. 4.90a, 4.90c, 4.91, and 4.92) that the work/energy equation for the system is

$$\frac{dE}{dt} = \sum_{i=1}^{3} L_i\,\omega_i + \frac{I_2^*}{J_2}\,h_2\,u \tag{4.95}$$

from which we conclude that total energy is a constant, if $L_i(t) = 0$ and either $h_2(t) = 0$ or $u(t) \equiv 0$. The latter condition corresponds to the "free-wheeling"

case of no motor torque, and the former to the wheel locked case (in this event, the two body system clearly becomes a single composite rigid body).

Let us consider the stability of the "free wheeling" case. If external torque is negligible, Eqs. 4.90a, 4.90b, and 4.91 for motion near the equilibrium state

$$\omega_1 = \omega_o$$
$$\omega_1 = \omega_2 = 0$$
$$h_2 = h$$

using the small departure approximations

$$\omega_1 \cong \dot{\phi} + \omega_o\psi$$
$$\omega_2 \cong \dot{\theta} + \omega_o \quad , \quad h_2 = h + \delta$$
$$\omega_3 \cong \dot{\psi} - \omega_o\phi$$

reduces the equation of motion to the linear equations

$$\textit{Roll:} \quad 0 = I_1\ddot{\phi} + \omega_o[(I_2 - I_3)\omega_o + h]\phi + (\omega_o\beta - h)\dot{\psi} \tag{4.96a}$$

$$\textit{Pitch:} \quad 0 = I_2\ddot{\theta} + \dot{\delta} \tag{4.96b}$$

$$\textit{Yaw:} \quad 0 = I_3\ddot{\psi} + \omega_o[(I_2 - I_1)\omega_o + h]\psi - (\omega_o\beta - h)\dot{\phi} \tag{4.96c}$$

It is obvious that the pitch motion (rotation about $\hat{b}_2$ which is also the rotor axis), is uncoupled from roll/yaw and, we conclude $I_2\dot{\theta} + \delta$ is a constant; a small perturbation in $(\theta, \dot{\theta})$ does not grow large unless the wheel momentum variation $\dot{\delta}$ is nonzero. It is evident from $h_2 = h + \delta$ and Eq. 4.92 that $\dot{\delta} = 0$; we therefore conclude $\dot{\theta}$ = constant. If the pitch motion is to be "stable", we require a restoring torque, such as due to gravity gradient. The roll/yaw equations are coupled and have the associated characteristic equation

$$\lambda^4 + a_1\lambda^2 + a_2 = 0 \tag{4.97}$$

with

$$a_1 = \frac{1}{I_1I_3}\{(\omega_o\beta - h)^2 + \omega_oI_1[\omega_o(I_2 - I_1) + h] + \omega_oI_3[\omega_o(I_2 - I_3) + h]\} \tag{4.98}$$

$$a_2 = \frac{\omega_o^2}{I_1 I_3}[\omega_o(I_2 - I_3) + h][\omega_o(I_2 - I_1) + h] \tag{4.99}$$

Requiring the coefficients of Eq. 4.97 to be non negative (to guarantee non-divergent solutions for ϕ and ψ) yields the asymmetric dual spin stability necessary conditions

$$\begin{matrix}\textit{dual-spin} \\ \textit{stability} \\ \textit{conditions}\end{matrix}\begin{cases} h + \omega_o(I_2 - I_3) \geq 0 \\ h + \omega_o(I_2 - I_1) \geq 0 \end{cases} \tag{4.100}$$

Thus, regardless of whether $\hat{b}_2$ is the axis of largest, least, or intermediate inertia, we can find lower bounds on wheel momentum from Eq. 4.100. It is a relatively minor modification to the above discussion to include the gravity gradient torque of Eq. 4.58 and thereby generalize the gravity gradient results of Section 4.3 to reflect a vehicle which contains a rotor aligned with one of its principal axes. The resulting equations of motion are

$$\textit{Roll:} \quad I_1 \ddot{\phi} = -\omega_o[4\omega_o(I_2 - I_3) + h]\phi + [h - \omega_o\beta]\dot{\psi} \tag{4.101a}$$

$$\textit{Pitch:} \quad I_2^* \ddot{\theta} = -3\omega_o^2(I_1 - I_3)\theta \tag{4.101b}$$

$$\textit{Yaw:} \quad I_3 \ddot{\psi} = -\omega_o[\omega_o(I_2 - I_1) + h]\psi - [h - \omega_o\beta]\dot{\phi} \tag{4.101c}$$

By inspection, the pitch motion is oscillatory if $I_1 \geq I_3$, consistent with Eq. 4.65 for a rigid vehicle without a rotor. The roll/yaw characteristic equation remains of the form in Eq. 4.97, but the coefficients, revised to reflect $h \neq 0$ are

$$\alpha_1 = \frac{1}{I_1 I_3}\{(h - \omega_o\beta)^2 + \omega_o I_1[\omega_o(I_2 - I_1) + h] + \omega_o I_3[4\omega_o(I_2 - I_3) + h]\} \tag{4.102a}$$

$$\alpha_2 = \frac{\omega_o^2}{I_1 I_3}[\omega_o(I_2 - I_1) + h][4\omega_o(I_2 - I_3) + h] \tag{4.102b}$$

Requiring $\alpha_i > 0$ for stability gives the dual-spin/gravity gradient stability necessary conditions:

$$h + 4\omega_o(I_2 - I_3) \geq 0$$

$$h + \omega_o(I_2 - I_1) \geq 0 \tag{4.103}$$

Notice, comparing Eq. 4.103 with Eq. 4.100, that the presence of the gravity gradient torque has the effect of requiring a greater bias momentum. Typically, the bias momentum is much larger than the minimum bound implied by Eq. 4.103, to offset disturbance torques. We still require $I_3 \leq I_1$ for pitch stability, but I_3 may not necessarily be the axis of least inertia so long as conditions of Eq. 4.103 are satisfied.

Recently, Li and Longman (ref. 10) have considered the dynamics of dual spin configurations with the rotor allowed to assume an arbitrary body fixed orientation, (i.e., not necessarily colinear with a principal axis). Including the effects of graivty gradient torques and constraining attention to a circular orbit, they find an infinity of equilibrium states, and establish as a function of inertias and orbit parameters the optimum body fixed orientation to maximize stiffness of the stable orientation equlibrium state with respect to disturbance torques.

4.4.2 Maneuvers of a Dual Spin Configuration

A dual spin problem of recent interest (Barba and Aubrun, ref. 11), (Gebman and Mingori, ref. 12), (Vigneron, ref. 13), (Cochran and Junkins, ref. 14), and (Kaplan, ref. 15) is the family of large non-linear maneuvers achievable by transferring angular momentum from an asymmetric spacecraft to a rotor aligned with one of its principal axes.

In particular, consider the initial conditions

$$\begin{aligned} \omega_3 &= \omega_{30} >> 0 \\ \omega_1 &= \omega_2 = 0 \\ h_2 &= h = 0 \end{aligned} \tag{4.104}$$

The body is initially spining uniformly about the $\hat{b}_3$ principal axis with the rotor locked. It is evident from Eq. 4.89 to 4.91 that if $\dot{h}_2 = \dot{h} = 0$, the body will remain in pure spin. For simplicity, let the wheel relative momentum

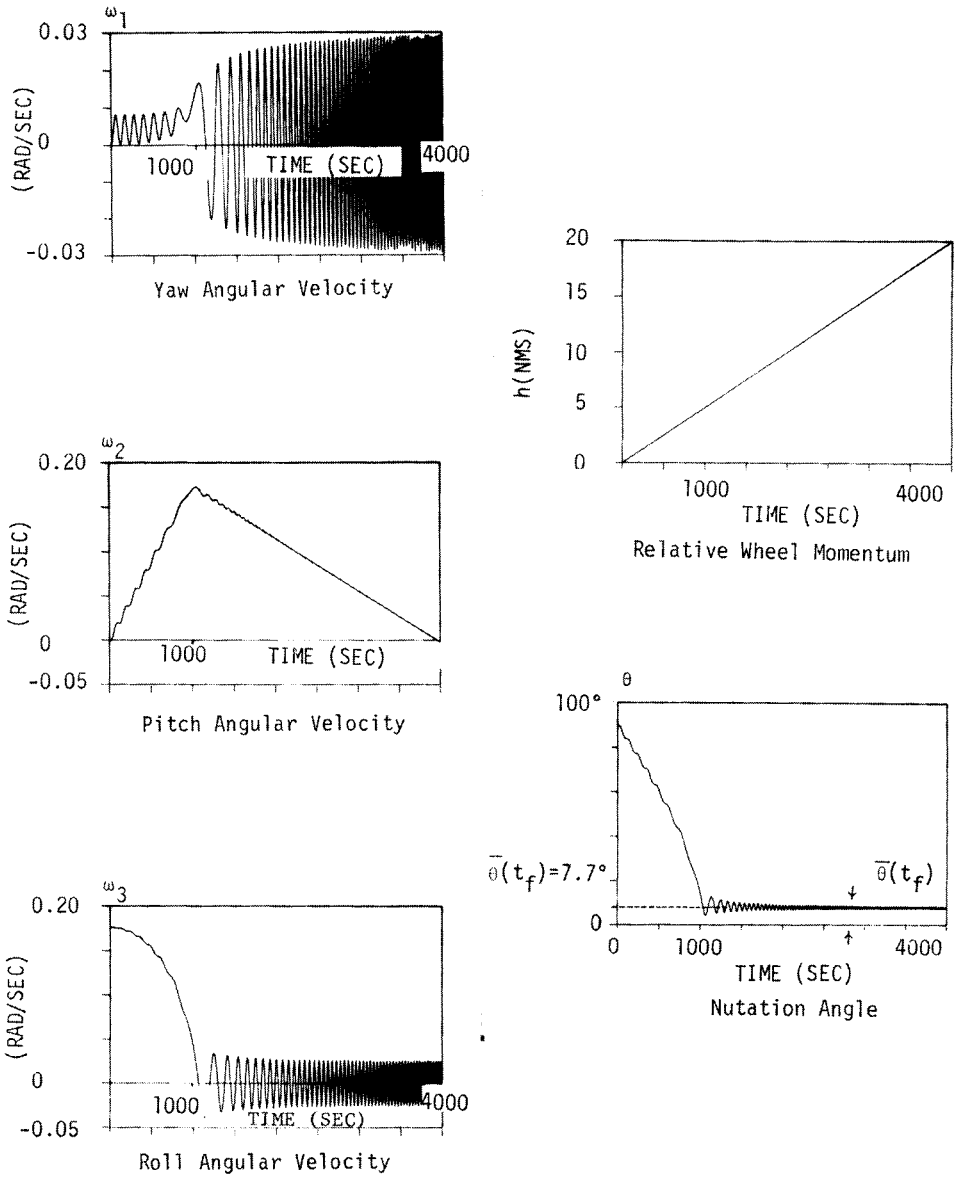

Figure 4.8 Flat Spin Recovery of a Dual Spin Spacecraft: The Maneuver of Barba and Aubrun

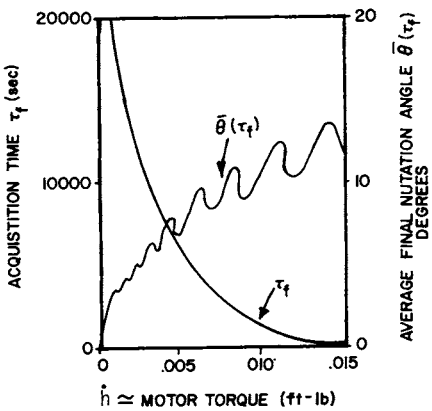

Figure 4.9 Residual Angle and Acquisition Time Versus $\dot{h}$

increase linearly so that

$$\dot{h} = C, \text{ a constant} \tag{4.105}$$

It is evident from solutions of Eq. 4.89 that the initial conditions in Eq. 4.104 are the departure state for some general motion which depends upon C, ω_{30}, and the inertia parameters of the system. In the absence of external torques, $L_1 = L_2 = L_3 = 0$, we know from Eq. 3.25 that the total angular momentum vector remains fixed in inertial space. We might conjecture that all of the angular momentum could be transferred from the body B into the rotor. If it is possible to transfer all of B's momentum to the rotor, the final state of the system is obvious; the body $\hat{b}_2$ axis must have rotated by 90° so that the rotor spins about the inertially fixed angular momentum vector while B is at rest with $\hat{b}_2$ along H. We might also suspect that such an ideal momentum transfer can only be carried out approximately; the degree to which all the

angular momentum can actually be transferred must depend upon the inertia parameters and, of course, ω_{30} and C.

Results of a Runge-Kutta numerical solution of Eq. 4.89 are shown in Figures 4.8 and 4.9. At first glance, these results are unusual and the underlying phsyics are not intuitively obvious. Observe that θ is the angle between $\hat{\mathbf{b}}_2$ and the inertially fixed angular momentum vector **H**; $\theta(t)$ does indeed decrease from the initial 90° error to small oscillations about a bias angle of about 7.7°. The oscillations begin around 1000 sec and approach constant amplitude oscillations about a constant mean value, with increasing frequency. The $\hat{\mathbf{b}}_2$ component $\omega_2(t)$ of angular velocity on the other hand, oscillates about an apparent positive-sloped straight line until around 1000 sec, at which instant, the slope abruptly becomes negative until ω_2 goes negative at 4000 sec. On the other hand, $\omega_3(t)$ oscillates about a decreasing parabolic shaped function until about 1000 sec, at which time it begins oscillating about zero with increasing frequency. The residual angle (θ_0), and time t_A (4000 sec in the above example) depend upon the system parameters in a complicated way, but considered as a function of $\hat{h} = C$ alone, they behave as shown in Figure 4.9. We conclude that if $\hat{h} = C$ is sufficiently small, we can perform the 90° attitude maneuver with negligible final error, but an unacceptably long associated maneuver time may result.

In order to gain some physical insight to the above motion, Barba and Auburn (ref. 11) introduced a variation of the ideas underlying the energy momentum surface intersections of Section 4.2. Consider the total energy as given by Eq. 4.94. Barba and Auburn deleted the last two terms (those which reflect the contributions due to rotor spin) and defined

$$E^* = \frac{1}{2}\left(I_1\,\omega_1^2 + I_2\,\omega_2^2 + I_3\,\omega_3^2\right) \tag{4.106}$$

Clearly E^* is a positive measure of the system's motion excluding the rotor spin; in particular if body B is brought to rest, it is evident that E^* goes to

zero. Conversely, if we control the motor torque in such a fashion that we drive E* to zero, we must necessarily bring the spacecraft to rest, i.e., all of the system angular momentum (and energy) must necessarily be absorbed into spin of the rotor about the inertially fixed angular momentum vector, since E* is a positive definite function of B's angular velocity. It is easily verified, by differentiation of Eq. 4.106 and substitution for the $\dot{\omega}_i$ from Eqs. 4.89, and for $L_i = 0$, $\dot{h} = C$, that

$$\frac{dE^*}{dt} = - C\, \omega_2(t) \tag{4.107}$$

From Eq. 4.107 we conclude that, if C = 0, E* given by Eq. 4.106 becomes an integral of the motion. If C is constant, it is evident that the instantaneous signs of C and $\omega_2(t)$ dictates whether the energy E*(t) is increasing or decreasing. Since external torques are assumed zero in this discussion, we can write the momentum sphere equation

$$H^2 = H_1^2 + H_2^2 + H_3^2 \tag{4.108}$$

which, as can be verified from Eqs. 4.85, 4.88, 4.89, is a rigorous integral of the motion. If C is set to zero, regardless of the instantaneous momentum stored in the rotor, it is evident that both E* and H remain constant and the angular momentum must lie on the intersection curve of the E* and H surfaces. In order to discuss the intersection curves, it is useful to eliminate the ω_i's in E* (Eq. 4.106) in favor of the H_i's; this is accomplished by rearranging Eq. 4.85 as

$$\begin{aligned} I_1\omega_1 &= H_1 \\ I_2\omega_2 &= H_2 - h \\ I_3\omega_3 &= H_3 \end{aligned} \tag{4.109}$$

and substituting into Eq. 4.106 so that the instantaneous energy surface becomes

$$1 = \frac{H_1^2}{2I_1E^*} + \frac{(H_2-h)^2}{2I_2E^*} + \frac{H_3^2}{2I_3E^*} \tag{4.110}$$

Thus the energy is an ellipsoid with semi axes $\sqrt{2I_i E^*(t)}$, and E^* evolves according to the differential Eq. 4.107. Clearly the geometrical center of the energy ellipsoid lies at $h = Ct$ on the $\hat{b}_2$ axis.

The angular momentum vector $\mathbf{H} = H_1 \hat{b}_1 + H_2 \hat{b}_2 + H_3 \hat{b}_3$ locates a point on the instantaneous intersection of the energy surface of Eq. 4.110 with the momentum sphere of Eq. 4.108. It is useful to remind ourselves that $\mathbf{H}$ is inertially fixed, its variation, when projected onto B-fixed axes $\hat{b}_i$, is due to B's angular motion. However, the time behavior of instantaneous angles

$$\theta_i = \cos^{-1}(\mathbf{H} \cdot \hat{b}_i / H) = \cos^{-1}(H_i/H) \quad , \quad i = 1,2,3 \qquad (4.111)$$

between the angular momentum vector and the $\hat{b}_i$ axes is easily visualized on these intersection curves. Figure 4.10 shows a sequence of six "snapshots" of the instantaneous energy surface of Eq. 4.110 intersected with the fixed momentum sphere. It is evident that for small C and energy near $H^2/(2I_3)$, $\mathbf{H}$ describes paths (closed for $\dot{h} = C = 0$) near the $\hat{b}_3$ axis; thus the body is in a state of near pure spin about $\hat{b}_3$. As h increases (and E^* decreases, although this fact needs to be established based upon analysis of Eq. 4.107), the energy surface decreases in size and the center displaces a distance $h = Ct$ out the $\hat{b}_2$ axis. The intersection of the instantaneous E^* and H surfaces becomes increasingly "tear drop" shaped as is shown in Cases 2 and 3.

A critical condition clearly occurs at the instant (Case 3) for which

$$h + \sqrt{2I_2 E^*} = H \qquad (4.112)$$

is satisfied. Note Eq. (4.112) is a "sepratrix" condition, if $\dot{h} = C$ is maintained, all subsequent $\mathbf{H}$ trajectories the (E^* - H intersection curves) will circulate about the $\hat{b}_2$ axis. If the objective, as described above, is to align $\hat{b}_2$ with the inertially fixed $\mathbf{H}$ vector, Vigneron (ref. 13) suggests a torque switching strategy: *At the instant the condition in Eq. 4.112 becomes satisfied, simply stop torquing the motor to maintain* $\dot{h} = C =$ *constant, and begin torquing the motor to maintain* $h = J_2 \Omega = a$

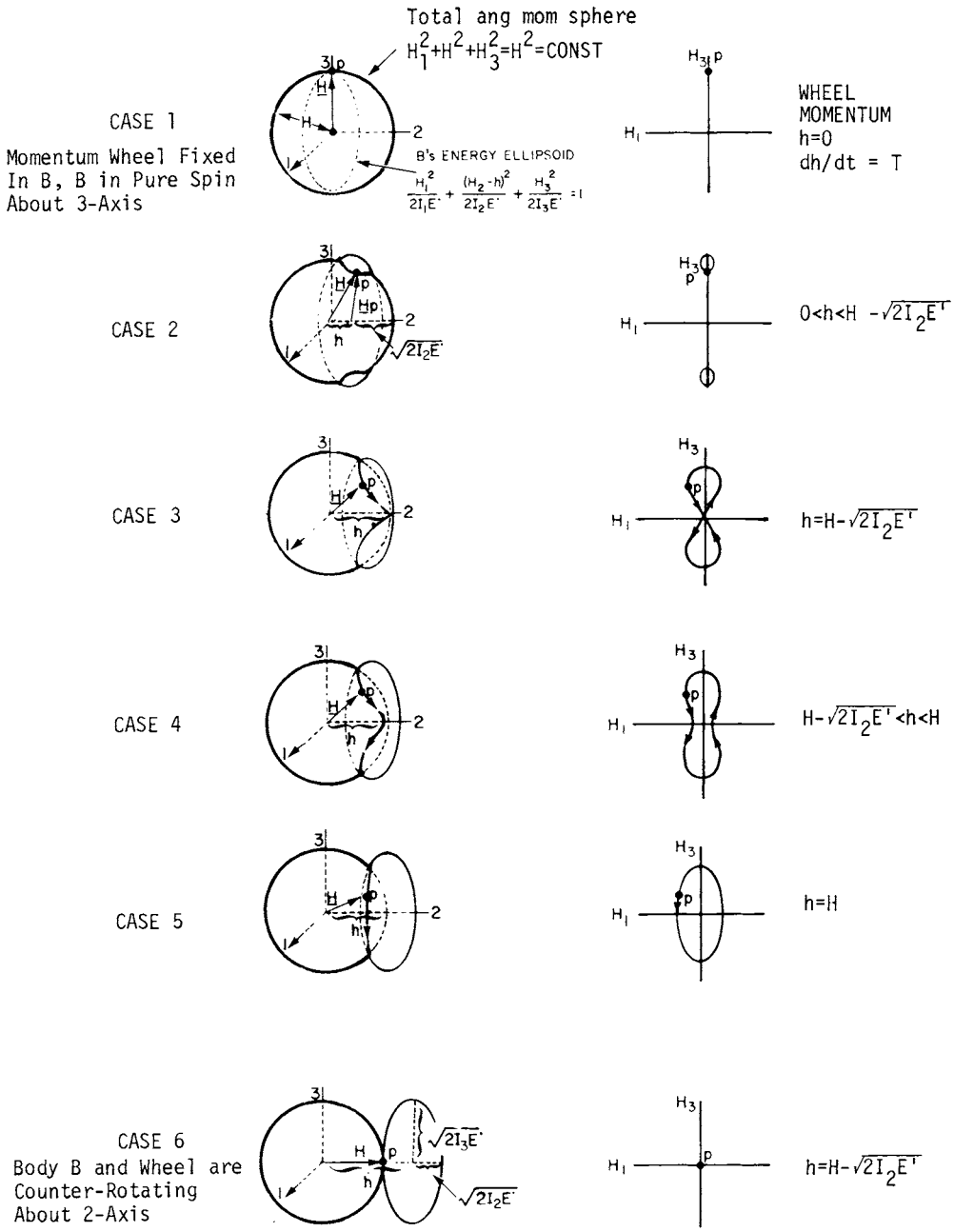

Figure 4.10 Intersection of the E^*- H Surfaces for a Dual Spin Spacecraft

constant ($\dot{h} = 0$). Note from Eq. 4.92, this does not mean that the motor torque is switched to zero. Physically, the spacecraft is still wobbling, we simply maintain a constant angular velocity of the rotor relative to the spacecraft. What is the consequence of this simple strategy? As is evident, the sepratrix motion terminates, eventually, with $\mathbf{H}$ aligned with $\hat{\mathbf{b}}_2$, as desired. Since this ideal situation will not be realized in practice (i.e., it is impossible to get *exactly* onto the sepratrix), we simply monitor $\theta = \theta_2(t)$ until it passes through a minimum and then re-initiate $\dot{h} = \pm C$ until Eq. 4.112 is satisfied again, based upon updated measurements. A passive damper can be used to null small final errors. If we do not employ the judicious switching as recommended in Reference 13, but simply maintain $\dot{h} = C$, as did Barba and Auburn in Reference 11, it is evident that another critical state (Case 5 of Figure 4.10) occurs when the condition

$$h = H \tag{4.113}$$

is reached at time $t^* = H/C$. Notice this is the instant for which the ellipsoid's (Eq. 4.110) geometric center lies on the surface of the sphere in Eq. 4.108. It is evident, without a formal proof, since angular momentum can be written as

$$\mathbf{H} = h\,\hat{\mathbf{b}}_2 + (I_1\,\omega_1\,\hat{\mathbf{b}}_1 + I_2\,\omega_2\,\hat{\mathbf{b}}_2 + I_3\,\omega_3\,\hat{\mathbf{b}}_3) \tag{4.114}$$

that the intersection curve lies to the left (for $h > H$) of the ellipsoid's geometrical center and, we infer

$$\omega_2(t) < 0$$

The exact instant that $\omega_2(t)$ first becomes negative requires rigorous analytical or numerical solutions, but it is obvious that this occurs before $t^* = H/C$. What is the significance of $\omega_2(t)$ being negative? From Eq. 4.107, it is obvious that the here-to-fore decreasing E^* now begins increasing and will increase indefinitely. Physically, $\omega_2(t) < 0$ means the torque $-u\,\hat{\mathbf{b}}_2$ acting on B is causing it to "counter rotate". The precise instant $t_A < t^* = H/C$ at

which counter rotation begins is defined as "acquisition time" by Barba and Auburn in Reference 11. Curiously, the ellipsoid moves to the right at a linear rate and it's axes grow at a rate which oscillates about linear. As a consequence, the curve of intersection does not change after time t*. However, **H** traverses the intersection curve at an increasing frequency. Returning to Figure 4.8 and studying it in conjunction with the first five cases of Figure 4.10, we see that the energy/momentum surface intersections provide an excellent geometrical device for anticipating and understanding these nonlinear motions. The sixth case is given just for completeness and corresponds to "perfect" counter rotation of the body about $-\hat{\mathbf{b}}_2$ and the wheel about $+\hat{\mathbf{b}}_2$.

Gebman and Mingori (ref. 12) constructed a matched asymptotic expansion perturbation solution for the above problem (matching of branched solutions "near $\hat{\mathbf{b}}_1$" and "near $\hat{\mathbf{b}}_3$" at the sepratrix condition). This analytical solution is rather elaborate, but does allow one to, for example, approximate t*, t_A, and the residual error in θ analytically in terms of the system inertias, initial conditions, and the parameter C.

In Chapter 8, we consider *optimal* momentum transfer maneuvers for the above configuration and a three wheel configuration. The present heuristic maneuver can be judged in the light of the optimal maneuvers in Section 8.3, to represent an easy-to-implement sub-optimal maneuver which is relatively near the solution which minimizes $\int_{t_0}^{t_f} u^2 dt$. We find in Chapter 8 that the optimal torque history, however, results in approximately a 50% reduction in $\theta(t_f)$.

4.4.3 Equations of Motion for an n-Rotor Spacecraft

We now consider a general asymmetric spacecraft (rigid body B) containing n symmetric wheels (ref. 16). The wheels may be used for momentum transfers for attitude stabilization, and/or reaction wheels for attitude maneuvers. The system S consists of a rigid body B and n symmetric wheels W_i whose axes are fixed in the body (Figure 4.11). The center of mass of the ith wheel is C_i and

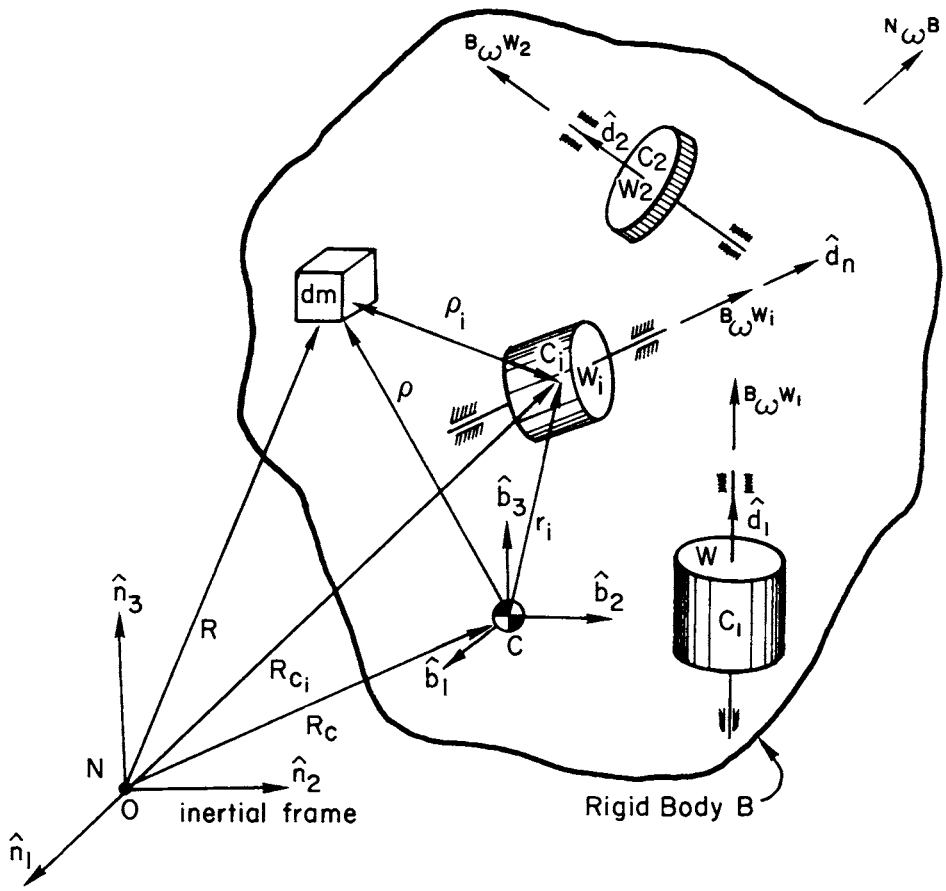

Figure 4.11 A General Multi-Spin Spacecraft Configuration

is arbitrarily located relative to C, the centroid of the system. Body fixed unit vectors are denoted $\{\hat{\mathbf{b}}\}$. The angular velocity of B relative to inertial space N is $^N\omega^B$. The angular velocity of W_i relative to B is $^B\omega^{W_i} = \Omega_i \hat{\mathbf{d}}_i$ where $\mathbf{d}_i$ is a unit vector along the spin/symmetry axis of W_i. The inertial angular velocity of wheel W_i is therefore

$$^{N}\omega^{W_i} = {}^{N}\omega^{B} + \Omega_i \hat{d}_i .$$

The general procedure we follow here for developing the rotational equations of motion is to set the net external torque equal to the time rate of change of angular momentum. We therefore begin by writing the angular momentum of the system:

$$N_H S/C = N_H B/C + \sum_{i=1}^{n} N_H W_i/C \tag{4.115}$$

where $^{N}H^{S/C}$ = the total angular momentum of the system about its centroid C

$$N_H B/C \equiv \int_B \rho \times \dot{\rho} dm \tag{4.116}$$

$$N_H W_i/C \equiv \int_{W_i} \rho \times \dot{\rho} dm \tag{4.117}$$

In order to carry out the differentiation, we must first find convenient forms, i.e., in terms of known intertias and angular velocities in body axes components, for the integrals in Eqs. 4.116 and 4.117.

From Figure 4.11 $\rho = r_i + \rho_i$, substitute this into Eq. 3.208 to obtain

$$N_H W_i/C = (r_i \times \dot{r}_i)\int_{W_i} dm + r_i \times \int_{W_i} \dot{\rho}_i dm - r_i \times \int_{W_i} \rho_i dm + \int_{W_i} (\rho_i \times \dot{\rho}_i) dm \tag{4.118}$$

Note that $\int_{W_i} \rho_i dm = 0$, since ρ_i is measured from the center of mass of the i'th wheel, we have

$$\int_{W_i} \dot{\rho}_i dm = 0 \quad , \text{ since } \int_{W_i} \dot{\rho}_i dm = \frac{d}{dt}\int_{W_i} \rho dm = \frac{d}{dt}(0) = 0$$

$$\int_{W_i} dm = M_{W_i}, \text{ the mass of i'th wheel}$$

and by definition, $\int_{W_i} (\rho_i \times \dot{\rho}_i) dm = {}^{N}H^{W_i/C_i}$, the angular momentum of the i'th wheel about its centroid. Equation 4.118 reduces to

$$N_H W_i/C = N_H W_i/C_i + M_{W_i} (r_i \times \dot{r}_i) \tag{4.119}$$

and the angular momentum of the system is (substitute Eq. 4.119 into Eq. 4.115);

$$N_H S/C = N_H B/C + \sum_{i=1}^{n} N_H W_i/C_i + \sum_{i=1}^{n} M_{W_i} (r_i \times \dot{r}_i) \tag{4.120}$$

In terms of angular velocity and moments of inertia, we have

$$\{{}^{N}H^{B/C}\} = [I^{B/C}]\{{}^{N}\omega^{B}\} \tag{4.121}$$

and

$$\{{}^{B}H^{W_i/C_i}\} = [I^{W_i/C_i}]\{{}^{N}\omega^{W_i}\} \tag{4.122}$$

where

$${}^{N}\boldsymbol{\omega}^{B} = {}^{N}\omega_1^{B}\,\hat{\mathbf{b}}_1 + {}^{N}\omega_2^{B}\,\hat{\mathbf{b}}_2 + {}^{N}\omega_3^{B}\,\hat{\mathbf{b}}_3 \tag{4.123}$$

$${}^{N}\boldsymbol{\omega}^{W_i} = {}^{N}\omega_1^{W_i}\,\hat{\mathbf{b}}_1 + {}^{N}\omega_2^{W_i}\,\hat{\mathbf{b}}_2 + {}^{N}\omega_3^{W_i}\,\hat{\mathbf{b}}_3 \tag{4.124}$$

$$\{{}^{N}H^{B/C}\} = \begin{Bmatrix} {}^{N}H_1^{B/C} \\ {}^{N}H_2^{B/C} \\ {}^{N}H_3^{B/C} \end{Bmatrix} = \text{the } \{\hat{\mathbf{b}}\} \text{ components of } {}^{N}H^{B/C}$$

$[I^{B/C}]$ a 3 x 3 inertia matrix of B about the mass center of S and measured in $\{\hat{\mathbf{b}}\}$ axes system is a constant matrix; and

$$\{{}^{N}H^{N_i/C_i}\} = \begin{Bmatrix} {}^{N}H_1^{W_i/C_i} \\ {}^{N}H_2^{W_i/C_i} \\ {}^{N}H_3^{W_i/C_i} \end{Bmatrix} = \text{the } \{\hat{\mathbf{b}}\} \text{ components of } {}^{N}H^{W_i/C_i}$$

$[I^{W_i/C_i}]$ a 3 x 3 inertia matrix of W_i about the mass center of W_i and is measured in axes parallel to $\{\hat{\mathbf{b}}\}$ and centered at C_i. Since W_i is symmetric and is spinning about the symmetry axis, the matrix is also constant.

We now consider the $(\mathbf{r}_i \times \dot{\mathbf{r}}_i)$ term of Eq. 4.120. The body axes coordinates of $\mathbf{r}_i$ are given by

$$\mathbf{r}_i = X_i\,\hat{\mathbf{b}}_1 + Y_i\,\hat{\mathbf{b}}_2 + Z_i\,\hat{\mathbf{b}}_3 \tag{4.125}$$

also

$$\dot{\mathbf{r}}_i = {}^{N}\boldsymbol{\omega}^{B} \times \mathbf{r}_i$$

therefore

$$\mathbf{r}_i \times \dot{\mathbf{r}}_i = \mathbf{r}_i \times ({}^{N}\boldsymbol{\omega}^{B} \times \mathbf{r}_i) = (\mathbf{r}_i \cdot \mathbf{r}_i){}^{N}\boldsymbol{\omega}^{B} - (\mathbf{r}_i \cdot {}^{N}\boldsymbol{\omega}^{B})\mathbf{r}_i \tag{4.126}$$

Substitution of Eq. 4.123 and Eq. 4.124 into Eq. 4.126 yields

$$(\mathbf{r}_i \times \dot{\mathbf{r}}_i) = [(Y_i^2 + Z_i^2)\,{}^N\omega_1^B - X_iY_i\,{}^N\omega_2^B - X_iZ_i\,{}^N\omega_3^B]\hat{\mathbf{b}}_1$$
$$+ [-X_1Y_i\,{}^N\omega_1^B + (X_i^2 + Z_i^2)\,{}^N\omega_2^B - Y_iZ_i\,{}^N\omega_3^B]\hat{\mathbf{b}}_2 \qquad (4.127)$$
$$+[-X_iZ_i\,{}^N\omega_1^B - Y_iZ_i\,{}^N\omega_2^B + (X_i^2 + Y_i^2)\,{}^N\omega_3^B]\hat{\mathbf{b}}_3$$

We now have all the terms of Eq. 4.120 in manageable form. Substitution of Eqs. 4.121, 4.122, and 4.127 into Eq. 4.120 gives

$$\{{}^N H^{S/C}\} = [I^{B/C}]\{{}^N\omega^B\} + \sum_{i=1}^{n} [I^{W_i/C_i}]\{{}^N\omega^{W_i}\}$$

$$+ \sum_{i=1}^{n} M_{W_i} \begin{bmatrix} (Y_i^2+Z_i^2) & -X_i\,Y_i & -X_i\,Z_i \\ -X_i\,Y_i & (X_i^2+Z_i^2) & -Y_i\,Z_i \\ -X_i\,Z_i & -Y_i\,Z_i & (X_i^2+Y_i^2) \end{bmatrix} \{{}^N\omega^B\} \qquad (4.129)$$

Recalling that ${}^N\boldsymbol{\omega}^{W_i} = {}^N\boldsymbol{\omega}^B + {}^B\boldsymbol{\omega}^{W_i} = {}^N\boldsymbol{\omega}^B + \Omega_i\,\hat{\mathbf{d}}_i$

or $\{{}^N\omega^{W_i}\} = \{{}^N\omega^B\} + \Omega_i\,\{\mathbf{d}_i\}$

where

$$\{\mathbf{d}_i\} = \begin{Bmatrix} d_{1i} \\ d_{2i} \\ d_{3i} \end{Bmatrix} = \text{the } \{\hat{\mathbf{b}}\} \text{ components of the unit vector } \hat{\mathbf{d}}_i \text{ along the spin axis of the i'th wheel,}$$

we can write Eq. 4.129 as

$$\{{}^N H^{S/C}\} = [I^*]\{{}^N\omega^B\} + [A]\{\Omega\} \qquad (4.130)$$

where,

$$[I] = [I^{B/C}] + \sum_{i=1}^{n} [I^{W_i/C_i}] + \sum_{i=1}^{n} M_{W_i} \begin{bmatrix} (Y_i^2+Z_i^2) & -X_i\,Y_i & -X_i\,Z_i \\ -X_i\,Y_i & (X_i^2+Z_i^2) & -Y_i\,Z_i \\ -X_i\,Z_i & -Y_i\,Z_i & (X_i^2+Y_i^2) \end{bmatrix}$$

$$[A] = \left[[I^{W_1/C_1}]\{\mathbf{d}_1\} \quad [I^{W_2/C_2}]\{\mathbf{d}_2\} \quad \ldots \quad [I^{W_n/C_n}]\{\mathbf{d}_n\} \right]$$

and

$$\{\Omega\} = \begin{Bmatrix} \Omega_1(t) \\ \vdots \\ \Omega_n(t) \end{Bmatrix}$$

Finally, setting the time derivative of Eq. 4.130 equal to the net external torque gives

$$L_{ex} = \frac{d}{dt}\left({}^{N}H^{S/C}\right)_N = \frac{d}{dt}\left({}^{N}H^{S/C}\right)_B + {}^{N}\omega^{B} \times {}^{N}H^{S/C}$$

which can be written in matrix form as

$$\{L\} = [I]\{\dot{\omega}\} + [\tilde{\omega}][I]\{\omega\} + [A]\{\ddot{\Omega}\} + [\tilde{\omega}][A]\{\dot{\Omega}\} \qquad (4.131)$$

where

$$\{L\} = \begin{Bmatrix} L_{ex_1} \\ L_{ex_2} \\ L_{ex_3} \end{Bmatrix} = \{\hat{b}\} \text{ components of the external torque}$$

and

$$[\tilde{\omega}] = \begin{bmatrix} 0 & -{}^{N}\omega_3^{B} & {}^{N}\omega_2^{B} \\ {}^{N}\omega_3^{B} & 0 & -{}^{N}\omega_1^{B} \\ -{}^{N}\omega_2^{B} & {}^{N}\omega_1^{B} & 0 \end{bmatrix}$$

As is evident by comparison of Eq. 4.131 with the matrix version Euler's Eq. 3.28 for a single rigid body, the dynamics of the spacecraft containing n rotors are of the same form, but has two additional *gyroscopic coupling terms* for $\{\Omega\}$ and $\{\dot{\Omega}\}$ non-zero. Contained as a near trivial special case of Eq. 4.131 are the dual spin equation of motion (Eqs. 4.89); obtained by considering Ω and $\dot{\Omega}$ scalars, $\{\hat{d}_1\} = [0\ 1\ 0]^T$, taking $[I]$ and $[I^{W_1/C_1}]$ as diagonal matrices, and setting $h_2 = I_2^{W_1/C_1}\Omega$.

Another case of particular interest in applications is the case of three identical, orthogonal reaction wheels, we wil consider this case in the optimal attitude maneuver discussions of Chapter 8.

REFERENCES

1. Morton, H. S., Jr., Junkins, J. L., **The Differential Equations of Rotational Dynamics**, Springer Verlag, in preparation.

2. Hubert, C., "The Use of Energy Methods in the Study of Dual-Spin Spacecraft," **Proc. of AIAA Guidance and Control Conference**, Danvers, MA., pp. 372-375, August 1980.

3. Hubert, C., "Spacecraft Attitude Acquisition from an Arbitrary Spinning or Tumbling State," **AIAA Journal of Guidance and Control**, Vol. 4, No. 2, pp. 164-170, March-April, 1981.

4. Junkins, J. L., Jacobson, I. D., and Blanton, J. N., "A Nonlinear Oscillator Analog of Rigid Body Dynamics," **Celestial Mechanics**, Vol. 7, pp. 398-407, 1973.

5. Meirovtich, L., **Methods of Analytical Dynamics**, McGraw-Hill, New York, 1970.

6. Routh, E. J., **Advanced Rigid Dynamics**, MacMillian and Co., London, 1892.

7. Blanton, J. N., **Some New Results on the Free Motion of Triaxial Rigid Bodies**, Ph.D. Dissertation, Univ. of Va., Aug. 1976.

8. Booth, R. J. **Tangential Coordinates: On the Application of a New Analytical Method to the Theory of Curves and Curved Shapes**, George Bell, London, 1877.

9. Junkins, J. L., Rajaram, S., Baracat, W. A., and Carrington, C. K., "Precision Autonomous Satellite Attitude Control Using Momentum Transfer and Magnetic Torquing," **Journal of the Astronautical Sciences**, Vol. XXX, No. 1, Jan. 1982.

10. Li, T., and Longman, R. W., "Optimal Configurations for Dual-Spin Satellites Subject to Gravitational Torques," to appear, **Celestial Mechanics**, Communicated Privately to J. L. Junkins, Oct., 1981.

11. Barba, P., and Aubrun, J., "Satellite Attitude Acquisition by Momentum Transfer," Paper #AAS-75-053, Presented at the AAS/AIAA Astrodynamics Conference, Nassau, Bahammas, July 1975.

12. Gebman, G. and Mingori, T., "Perturbation Solution for the Flat Spin Recovery of a Dual-Spin Spacecraft," **AIAA Journal**, Vol. 14, July 1976, pp. 859-867.

13. Vigneron, F. R., Private communication with J. L. Junkins, June 1981.

14. Cochran, J. E., and Junkins, J. L., "Large Angle Satellite Attitude Maneuvers," **Proceedings of the Flight Mechanics/Estimation Theory Symposium**, Goddard Space Flight Center, Greenbelt, MD., April 1975.

15. Kaplan, M., **Modern Spacecraft Dynamics and Control**, Wiley & Sons, N.Y., 1976.

16. Blanton, J. N., Unpublished Notes, developed in collaboration with J. L. Junkins, at the Univ. of Virginia, Entitled "Derivation of the Rotational Equations of Motion for a Rigid Body with N Symmetric Rotors," Dec. 1975.